REPORT No. 543

TANK TESTS OF N. A. C. A. MODEL 40 SERIES OF HULLS FOR SMALL FLYING BOATS AND AMPHIBIANS

By JOHN B. PARKINSON and JOHN R. DAWSON

SUMMARY

The N. A. C. A. model 40 series of flying-boat hull models consists of 2 forebodies and 3 afterbodies combined to provide several forms suitable for use in small marine aircraft. One forebody is of the usual form with hollow bow sections and the other has a bottom surface that is completely developable from bow to step. The afterbodies include a short pointed afterbody with an extension for the tail surfaces, a long afterbody similar to that of a seaplane float but long enough to carry the tail surfaces, and a third obtained by fitting a second step in the latter afterbody.

The various combinations were tested in the N. A. C. A. tank by the general method over a suitable range of loadings. Fixed-trim tests were made for all speeds likely to be used and free-to-trim tests were made at low speeds to slightly beyond the hump speed. The characteristics of the hulls at best trim angles have been deduced from the data of the tests at fixed trim angles and are given in the form of nondimensional coefficients applicable to any size of hull.

Comparisons among the forms are shown by suitable cross plots of the nondimensional data and by photographs of the spray patterns. The difference between the results obtained with the two forebodies was small for the smooth-water conditions simulated in the tank. With the same forebody in each case, the resistance of the no-step afterbody was least at the hump speed and that of the pointed afterbody was least at high speeds.

Take-off examples of an 8,000-pound flying boat or amphibian having a power loading of 13.3 pounds per horsepower and a 2,000-pound flying boat having a power loading of 18.2 pounds per horsepower are included to illustrate the application of the data.

INTRODUCTION

A "general" test of a given form of hull as made in the N. A. C. A. tank provides data for all speeds, loads, and trim angles for which the form is suitable. These data may be used to compare the water characteristics with those of other forms and to estimate the water performance of possible applications of the lines over a considerable range of full-size dimensions. The results of such tests on 11 forms have been published to date by the Committee.

The models tested have, in general, the forms found in a limited number of large flying boats. A need has been expressed for general test data regarding forms similar to those used on the smaller flying boats and amphibians of 2,000 to 10,000 pounds gross weight. The hulls of flying boats in this class appear to have higher length-beam ratios and higher beam loadings (C_Δ values) than are usual for the hulls of the larger craft thus far investigated. The amphibians also have higher angles of afterbody keel. Because the hulls are relatively narrow, a moderate angle of dead rise gives satisfactory shock-absorbing qualities and, because they are heavily loaded for their size, some means of suppressing spray such as hollow sections or spray strips is particularly desirable.

Simplicity of form seems to be a conspicuous feature of the designs in this class. Excessive flaring of the forebody sections requiring extensive forming of the plating is avoided; likewise, a simple form of afterbody is usually adopted. Because of the low power loadings generally employed, the compromises made among water and flight characteristics favor those of flight. These smaller craft are less seaworthy than the large flying boats but usually operate in inland waters, which do not demand the degree of seaworthiness necessary in the open sea.

The N. A. C. A. model 40 series of flying-boat hulls was designed with the foregoing considerations in mind. It includes 2 forebodies and 3 afterbodies in various combinations that are of interest to the designers of small marine aircraft. General tests of 5 of the 6 possible combinations were made in the N. A. C. A. tank during 1934. From the results of the tests, the water performance of full-size hulls having their lines may be estimated and the effect of changes in form within the limits covered by the series may be determined.

DESCRIPTION OF MODELS

LINES

General.—The lines developed for the series are shown in figures 1 and 2. The faired offsets for the models are given in tables I to IV. The following particulars apply to all the variations:

	Inches	Percentage of maximum beam
Forebody length	42.00	311.80
Over-all length	100.00	742.39
Beam over chine	13.00	96.51
Beam over spray strips	13.47	100.00
Depth	14.00	103.93
Width of spray strip	.25	1.86
Width of keel flat	.20	1.48
Depth of step	.50	3.71

Angle of dead rise, stations 6 and aft, 20°.

The V bottom cross section with the spray strip added at the chine was considered to be the most economical arrangement for this class of hull. In the tank, the water breaks cleanly from the edge of the strip before the hump speed is reached; hence this edge, rather than the chine, is considered to be the boundary of the bottom. It is suggested that in full-size applications the strip be extended to the bow.

Forebodies.—The length of the forebody was made as short as was thought to be practicable for the loadings intended in order to keep the structure forward of the portion of the hull that is used for passengers or cargo as light as possible. Forward of the step the planing bottom is longitudinally straight for good planing characteristics while farther forward the bottom

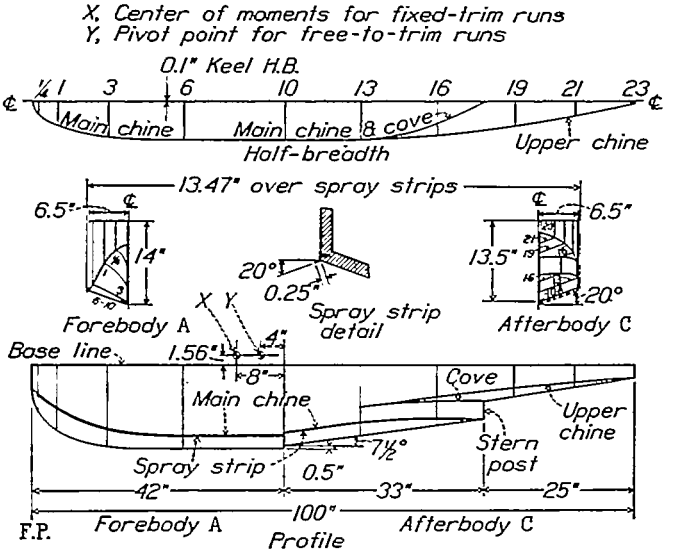

FIGURE 1.—Lines of forebody A and afterbody C.

rises sharply toward the bow. The bow sections of forebody A are slightly flared in the usual manner as an aid in meeting oncoming waves. The plan form of its chine is rounded at the bow to facilitate rounding the deck above it when desirable from aerodynamic considerations.

Forebody B was developed to be used where extreme simplicity of form is desirable. The bottom surface forward of the flat planing bottom is generated by a straight line moving parallel to itself with the chine as a directrix. The bottom surface is therefore that of a cylinder which may be unrolled into a flat sheet and

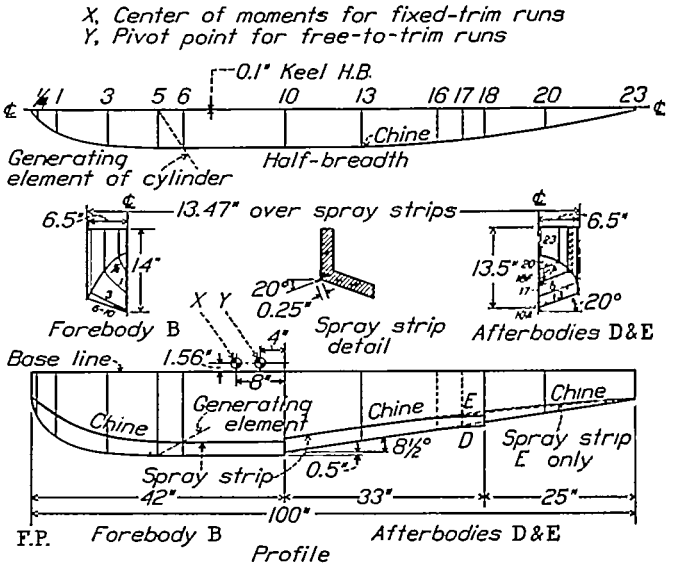

FIGURE 2.—Lines of forebody B, afterbody D, and afterbody E.

the entire surface of the hull is developable, no forming of the plating or planking being necessary in its construction. The slanting of the generating element in space as shown in figure 2 causes the angle of dead rise to increase toward the bow like that of the usual forms. As a result of this method of determining the surface, the conventional stations and water lines become slightly convex; hence, for practical applications, the use of a spray strip would be particularly desirable.

For the completely developable surface of forebody B, the plan form at the bow cannot be rounded but must be pointed so that the generating element will remain within the surface from keel to chine. Aft of station 6, forebodies A and B are identical.

Afterbodies.—Afterbody C is pointed in plan form and terminates in a narrow stern post. The extension of the hull, which carries the tail surfaces of the flying boat, is above the portion that is active during the take-off or immersed while at rest. The resulting form is an adaptation of the original NC type of afterbody, which has been favored by American designers. It is believed that the "cove" may be filleted with small effect on the water performance.

The angle of afterbody keel is made higher than that used on most large flying boats having this form of afterbody in order to provide a greater ground clearance for amphibians and to reduce high-speed resistance.

Afterbodies D and E provide second-step and no-step arrangements that are probably more economical

to construct than is a pointed type like afterbody C. The no-step afterbody is like that of a seaplane float and is much used in Europe for small craft. In some cases a second step is added to aid in controlling the trim angle at the hump speed or to provide additional lift while the afterbody is immersed. In afterbody D the portion ahead of the second step is curved down to give a higher effective trim angle for this portion of the bottom.

Combinations.—The forebodies and afterbodies were grouped for the tests as follows:

Model 40–AC: Normal forebody, pointed afterbody.

Model 40–AD: Normal forebody, second-step afterbody.

Model 40–AE: Normal forebody, no-step afterbody.

Model 40–BC: Developable forebody, pointed afterbody.

Model 40–BE: Developable forebody, no-step afterbody.

Tests of these combinations make it possible to compare the performances obtained when using the normal forebody with the three types of afterbody and when using the developable forebody with the pointed and no-step afterbodies. It was not considered necessary to test the developable forebody with the second-step afterbody as the characteristics of this combination may be inferred from the foregoing comparisons.

CONSTRUCTION

The various forebodies and afterbodies were constructed separately of mahogany to a tolerance of ± 0.02 inch and were bolted together at the step to form the combinations desired. In accordance with the usual practice at the N. A. C. A. tank, the surfaces were smoothly finished and given several coats of gray-pigmented varnish.

The spray strips were made of brass sheet 0.035 inch thick and 0.25 inch wide and were attached at the chines with wood screws through tabs formed on the strips at intervals. Unavoidable spaces between the inner edge of the strips and the model were filled with plasticine.

APPARATUS AND PROCEDURE

The N. A. C. A. tank and its testing apparatus are described in reference 1. The method of towing the model described therein introduced systematic errors because of the use of a "towing gate." The towing gate has been replaced by a counterbalanced girder as described in reference 2, and these errors are now eliminated. In the present towing gear the trimming moments are measured by a very stiff spring rigidly attached to the model. Water moments applied to the model cause the spring to deflect and the model to rotate slightly, but the deflections of the spring are so small that the change of trim angle due to the rotation of the model is within the limits of the accuracy to which the trim angle is set. The deflections of this spring are measured by a dial gage. The center of moments was arbitrarily placed at the point shown in figures 1 and 2.

The tests were made by the general method which consists of measuring resistance, trimming moment, and draft at a fixed trim angle for a number of loads throughout the speed range considered practicable. The trim angle is then changed and the procedure repeated until a sufficient number of trim angles are obtained to determine the trim angle that gives least resistance at each load and speed. The loads taken are expected to cover the useful range for the models tested.

At the lowest speeds the curves of resistance plotted against trim angle failed to show a minimum resistance within the range of trim angles at which it was possible to test these models. Instead, the resistance continued to decrease as the trim angle was increased. At speeds below the hump speed the resistance is generally of only minor interest in the take-off problem and it makes little difference whether minimum resistance is obtained or not. Since it is generally considered that in the average flying boat only a small amount of longitudinal control is available at low speeds, there is some justification for using free-to-trim (zero trimming-moment) resistance up to the hump when the values of the aerodynamic moments are unknown. Results from the general tests of these models showed, however, that, with the center of moments used in the tests, the free-to-trim resistance at very low speeds would be a great deal higher than the resistance encountered at the speed corresponding to the usual free-to-trim hump and would be even greater than the minimum hump resistance corresponding to best angle. Moving the center of gravity back toward the step would, of course, allow the model to trim at greater angles and thus reduce the free-to-trim resistance at low speeds.

Although the free-to-trim curves for any position of the center of gravity that does not produce trim angles outside the range of those tested may be determined from the general test data, it was decided to test all five models free to trim, up to and including the hump, with the center of gravity 4 inches forward of the step. These tests presented an opportunity to observe the free-to-trim performance of the models as well as to check the accuracy of zero trimming-moment curves obtained from the general test results.

RESULTS

GENERAL TEST DATA

The data obtained from the tests of the five combinations are plotted against speed in figures 3 to 32. The plotted resistance is the water resistance plus the air drag of the model and was obtained by deducting

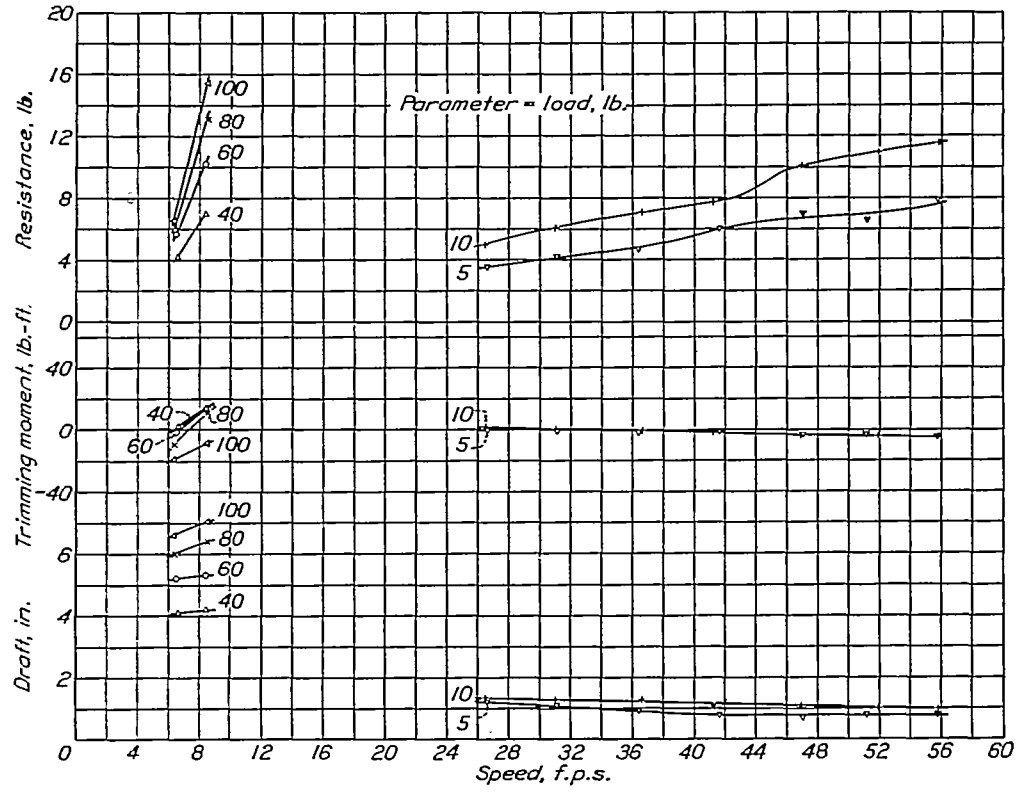

FIGURE 3.—Model 40-AC. Resistance, trimming moment, and draft. $\tau=2°$.

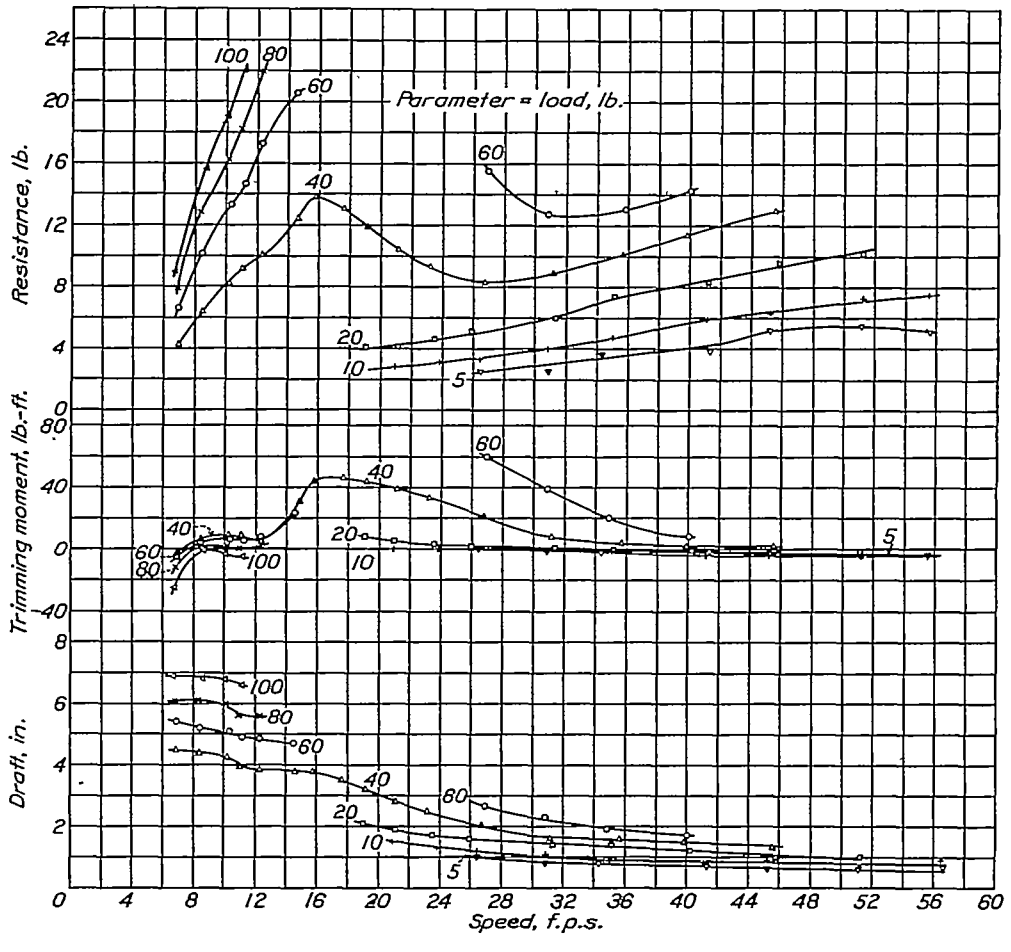

FIGURE 4.—Model 40-AC. Resistance, trimming moment, and draft. $\tau=3°$.

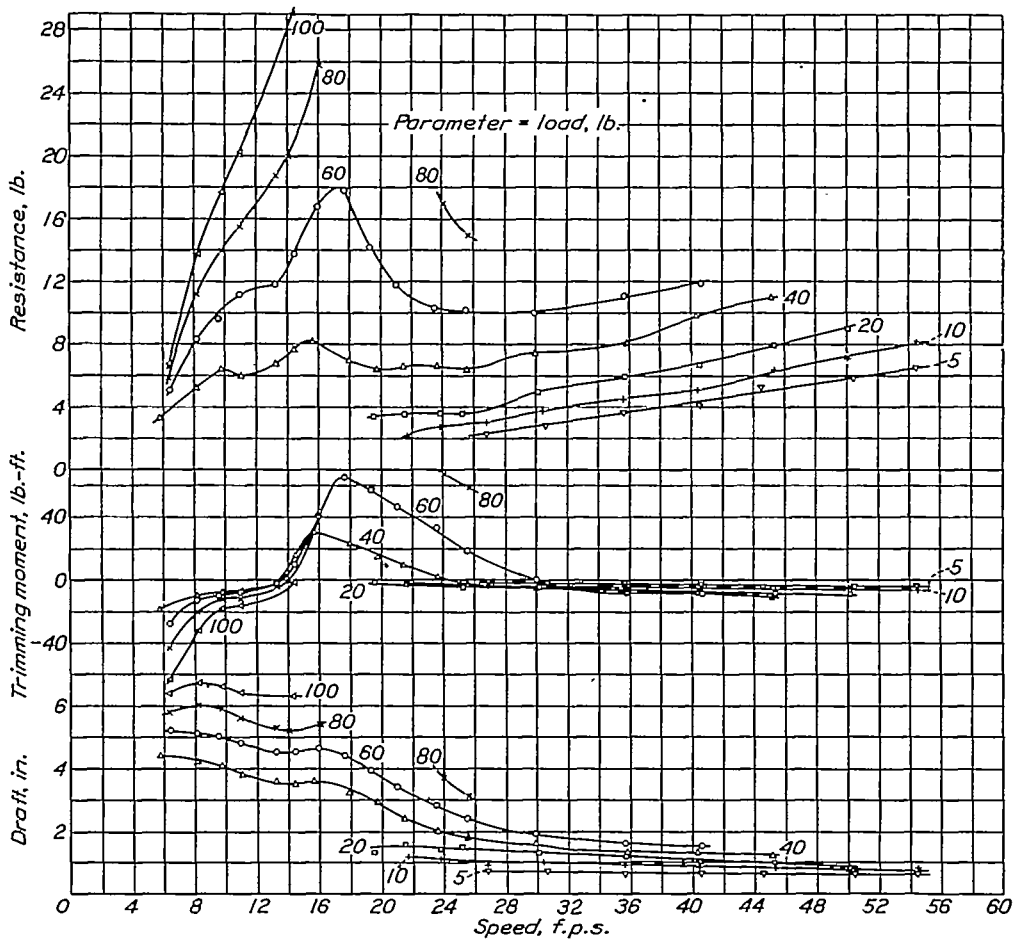

FIGURE 5.—Model 40-AC. Resistance, trimming moment, and draft. $\tau = 5°$.

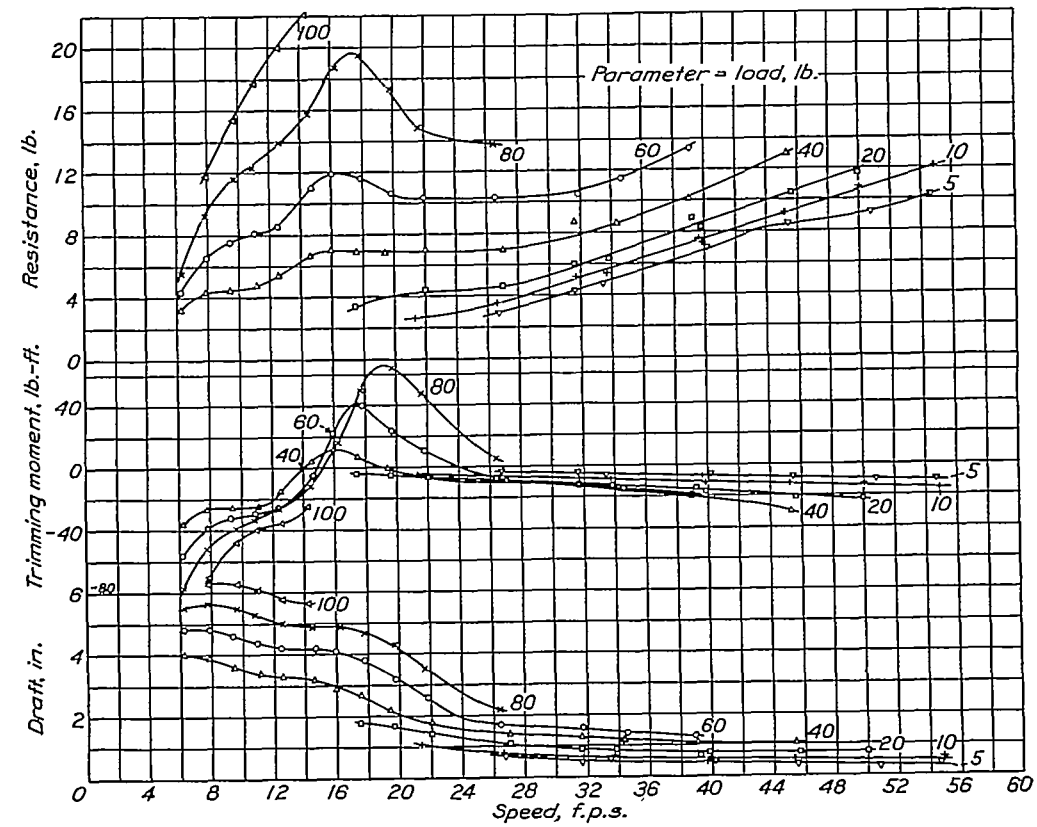

FIGURE 6.—Model 40-AC Resistance trimming moment, and draft $\tau = 7°$.

the air drag of the towing gear from the values weighed by the dynamometer. The trimming moments are referred to the center of moments shown in figures 1 and 2, which is 8 inches forward of the step. Positive moments tend to raise the bow. The drafts are the distances from the free-water surface to the keel at the main step. The main step is a convenient point of reference although the afterbody is deeper in the water at high angles of trim.

The exact conversion of trimming moments to the actual center of gravity used in a given design is laborious. The correction for a shift of the center of moments parallel to the base line for these hulls is given with sufficient accuracy, however, by the expression ΔX where Δ is the load on the water in pounds and X is the distance of the center of gravity aft of the center of moments in feet. At low speeds this simplification depends on the fact that the resultant-force vector is nearly equal in magnitude to its load component and the direction of the resultant force is nearly perpendicular to the base line at usual trim angles; at high speeds, although the resultant-force vector no longer has these properties, the absolute error introduced is small and may be neglected. The corrections for shift in the center of moments perpendicular to the base line will be small in the range of center-of-gravity positions usually encountered.

STATIC PROPERTIES

The trimming moments and drafts obtained with the models at rest in the tank are given in figures 33 to 37. The moments are referred to the same center of moments as that used in the fixed-trim tests, which is located 8 inches forward of the step. The drafts are measured from the free-water surface to the keel at the main step. The position of the load water line and the longitudinal stability at rest for a given application may be deduced from these curves without performing the extensive calculations necessary to obtain this information from the lines.

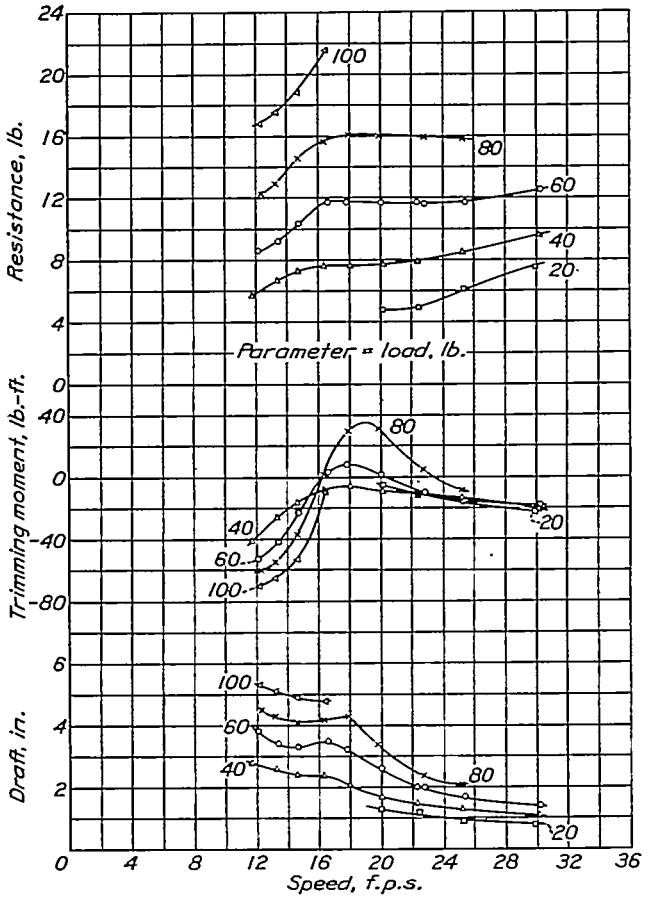

FIGURE 7.—Model 40-AC. Resistance, trimming moment, and draft. $\tau=9°$.

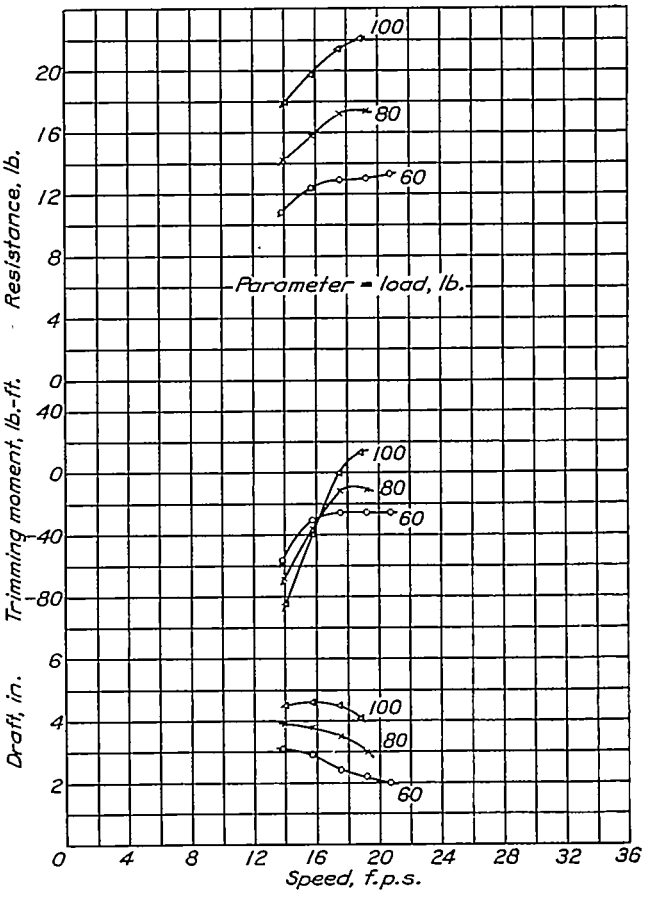

FIGURE 8.—Model 40-AC. Resistance trimming moment, and draft. $\tau=11°$.

The center of gravity of most seaplanes will be aft of the center of moments to which the trimming moments at rest are referred. Where the difference in height is small, the trimming-moment correction is approximately $\Delta_0 X$, where Δ_0 is the displacement and X is the distance of the center of gravity aft of the center of moments parallel to the model base line. Using this correction for an abscissa shift on the trimming-moment curves, the trim angle at rest for each load parameter may be read directly. A cross plot of these trim angles against load will enable the trim at the designed load to be determined. The draft at this trim being read from the draft curves, the water line for the assumed conditions may be drawn on the hull profile.

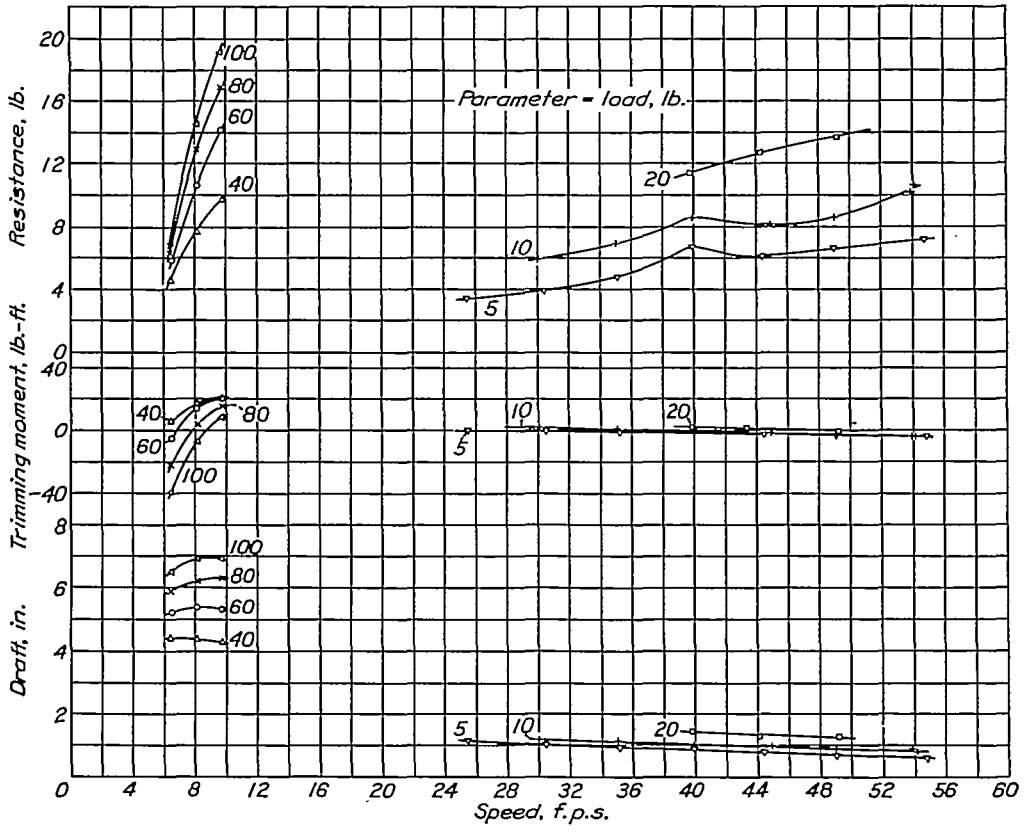

FIGURE 9.—Model 40-AD. Resistance, trimming moment, and draft. $\tau=2°$.

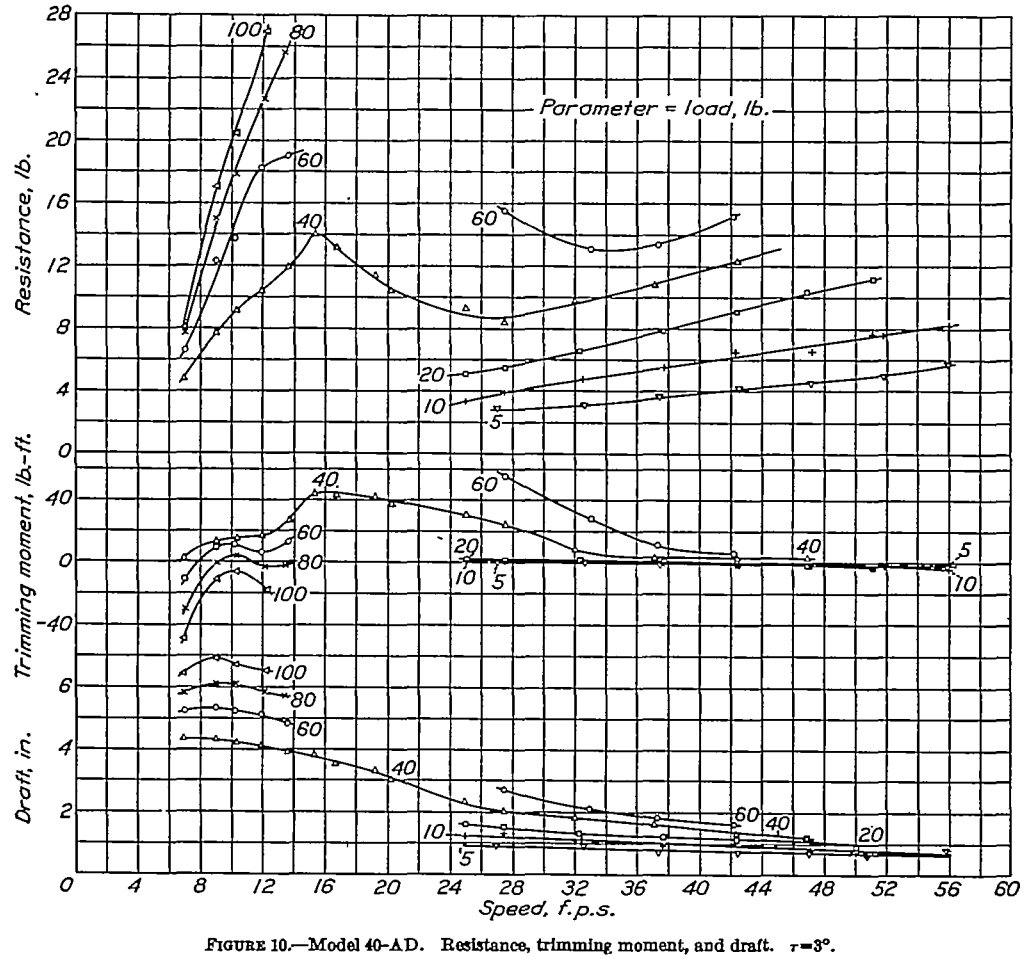

FIGURE 10.—Model 40-AD. Resistance, trimming moment, and draft. $\tau=3°$.

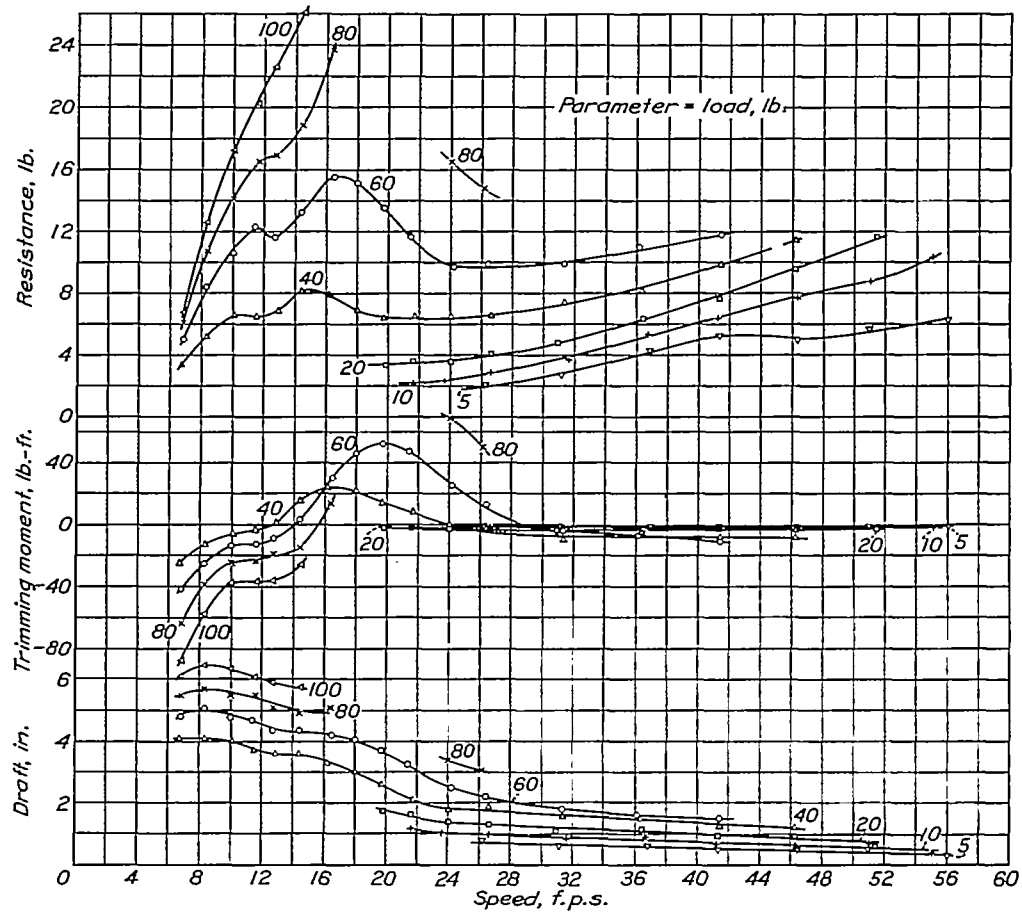

FIGURE 11.—Model 40-AD. Resistance, trimming moment, and draft. $\tau=5°$.

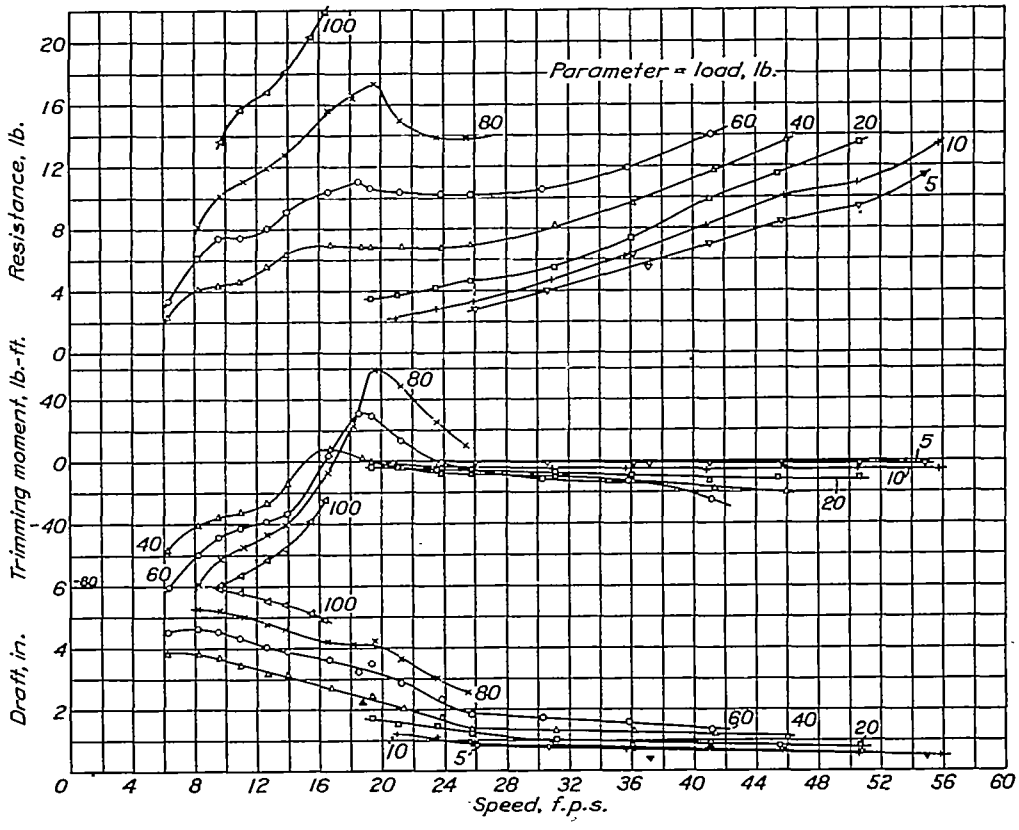

FIGURE 12.—Model 40-AD. Resistance, trimming moment, and draft. $\tau=7°$.

BEST-ANGLE DATA

The characteristics of the hulls as given in the curves of figures 3 to 32 are for three independent variables—speed, load, and trim angle. As it is desirable for a hull to remain near its best angle of trim and there is, in general, one angle for minimum resistance at each speed and load, it has been found desirable to derive the hull characteristics at best trim angle throughout the speed range. The trim-angle variable is thus eliminated and the optimum performance of the hull is determined.

The procedure consists of plotting the resistance and trimming moment for each load parameter against trim angle at a series of speeds. From these cross plots the minimum resistance, the best trim angle, and the trimming moment existing at that angle are determined for each load and speed. The data found are then converted to nondimensional coefficients, based on Froude's law of comparison and using the maximum beam over the spray strips as the characteristic dimension. The coefficients are defined as follows:

Speed coefficient, $C_V = \frac{V}{\sqrt{gb}}$

Load coefficient, $C_\Delta = \frac{\Delta}{wb^3}$

Resistance coefficient, $C_R = \frac{R}{wb^3}$

Trimming-moment coefficient, $C_M = \frac{M}{wb^4}$

where

V is speed, f. p. s.
Δ, load on the water, lb.
R, water resistance plus air drag of hull, lb.
M, trimming moment, lb.–ft.
b, beam over spray strips, ft.
g, acceleration of gravity, 32.2 ft. per sec.^{2}
w, specific weight of water, lb. per cu. ft.

NOTE: w was 63.5 lb. per cu. ft. during the tests and is usually taken as 64 lb. per cu. ft. for sea water.

The results of the best-angle analysis are given as curves of C_R against C_V in figures 38 to 42, C_R against C_Δ in figures 43 to 47, best trim angle, τ_0 against C_V in figures 48 to 52, and C_M against C_V in figures 53 to 57. The application of these curves in the determination of the take-off characteristics of a seaplane using the hull to which they refer is described in detail in reference 3.

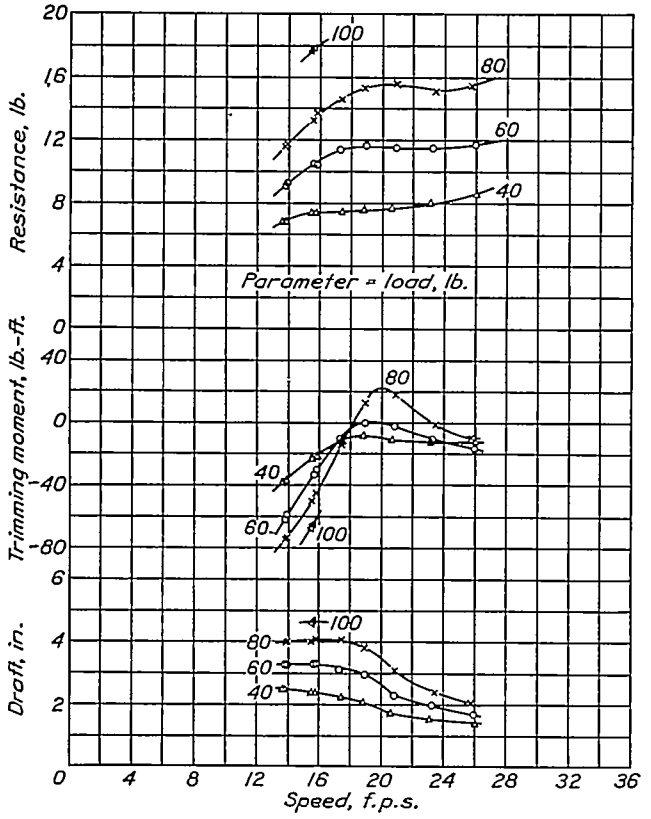

FIGURE 13.—Model 40-AD. Resistance, trimming moment, and draft. $\tau = 9°$.

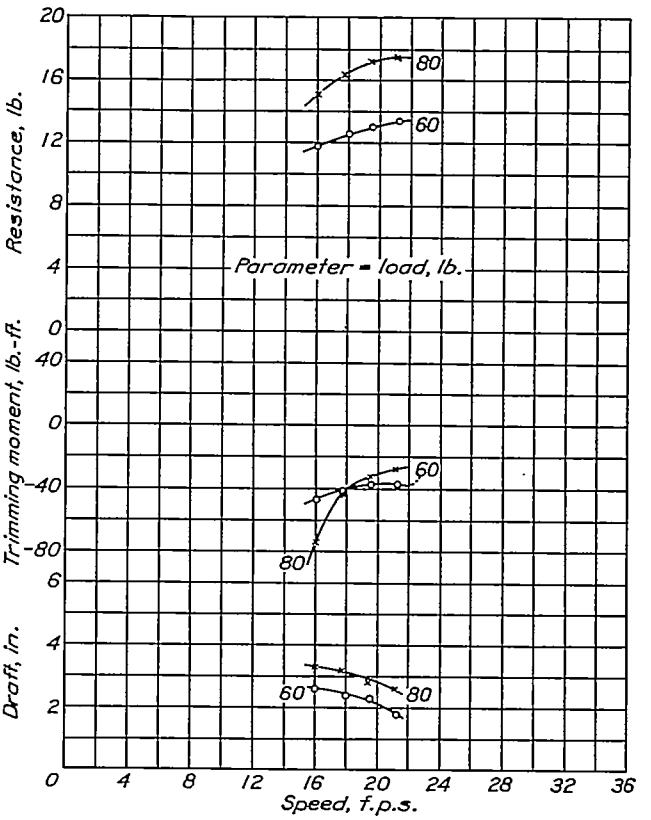

FIGURE 14.—Model 40-AD. Resistance, trimming moment, and draft. $\tau = 11°$.

FREE-TO-TRIM DATA

For speed coefficients below 2.0, the resistance continues to decrease with increase in trim angle, the best angles being above any practical range. As soon as the best angle is determinate, the trimming moments existing are found to have a high negative value but to decrease rapidly with speed until they become positive at the hump speed. The performance at low speeds is then best investigated by assuming the hull to be free to trim, as previously explained, or to be under the influence of the nearly constant thrust moment.

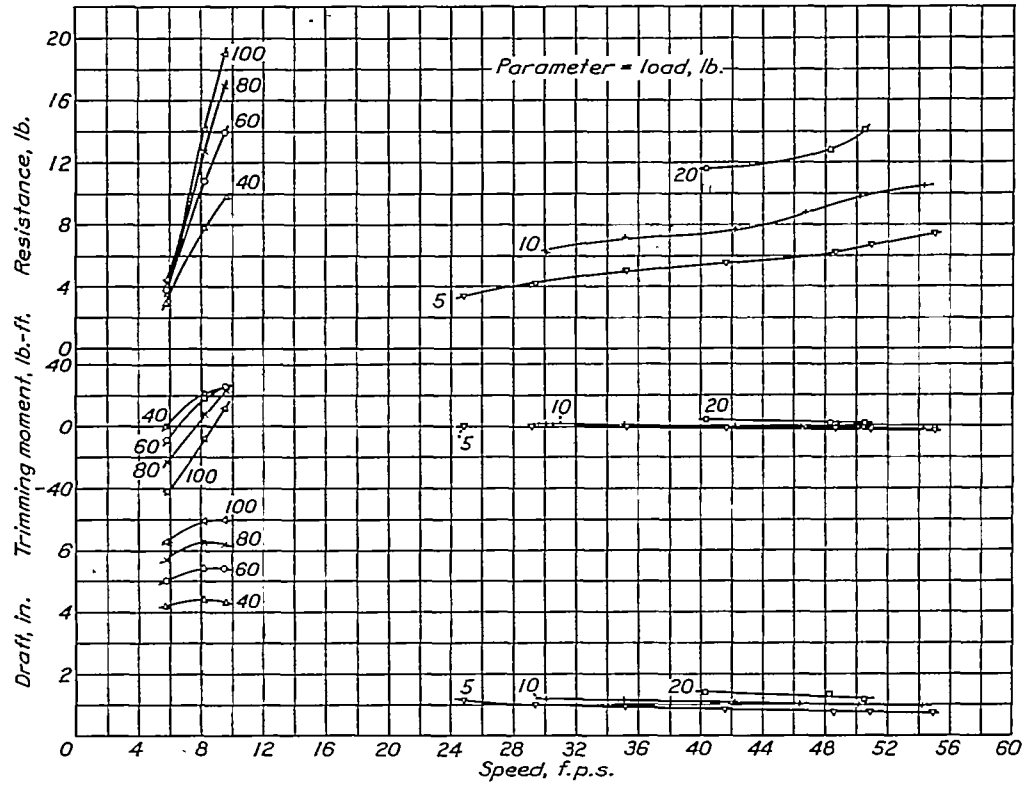

FIGURE 15.—Model 40-AE. Resistance, trimming moment, and draft. $\tau=2°$.

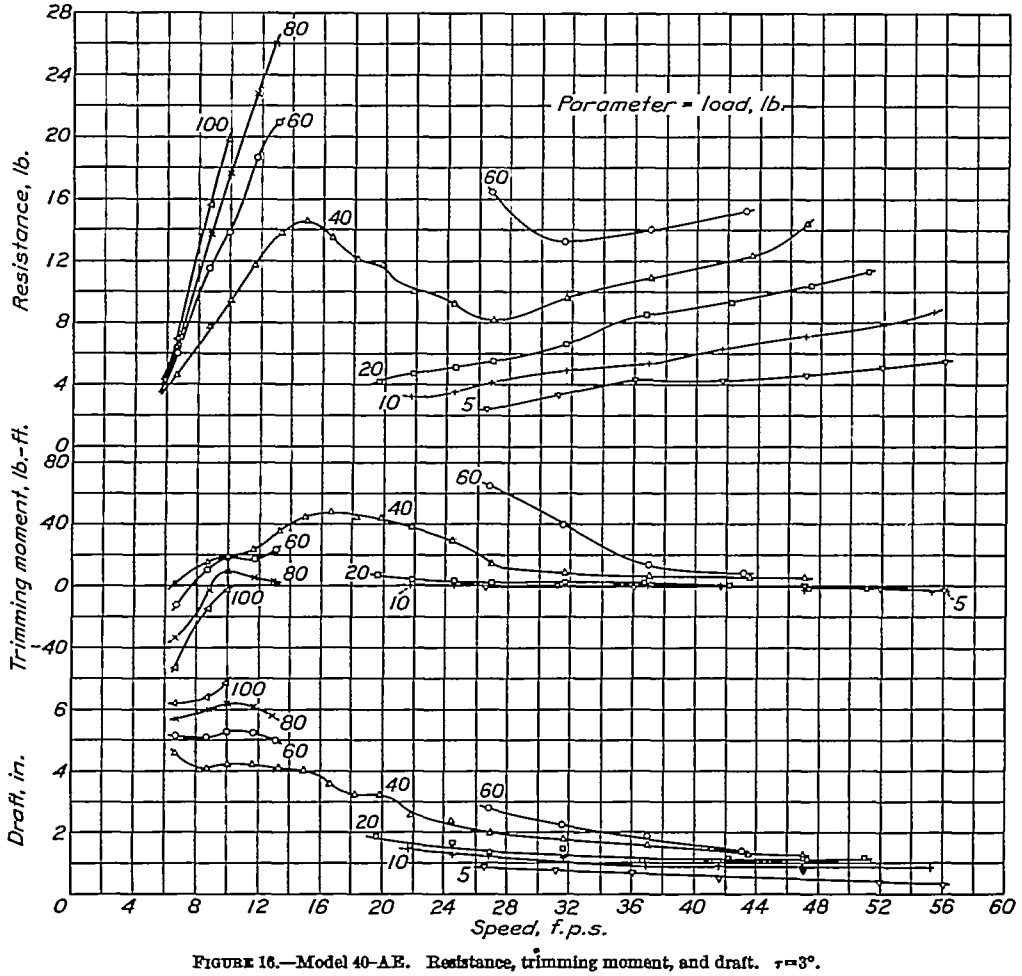

FIGURE 16.—Model 40-AE. Resistance, trimming moment, and draft. $\tau=3°$.

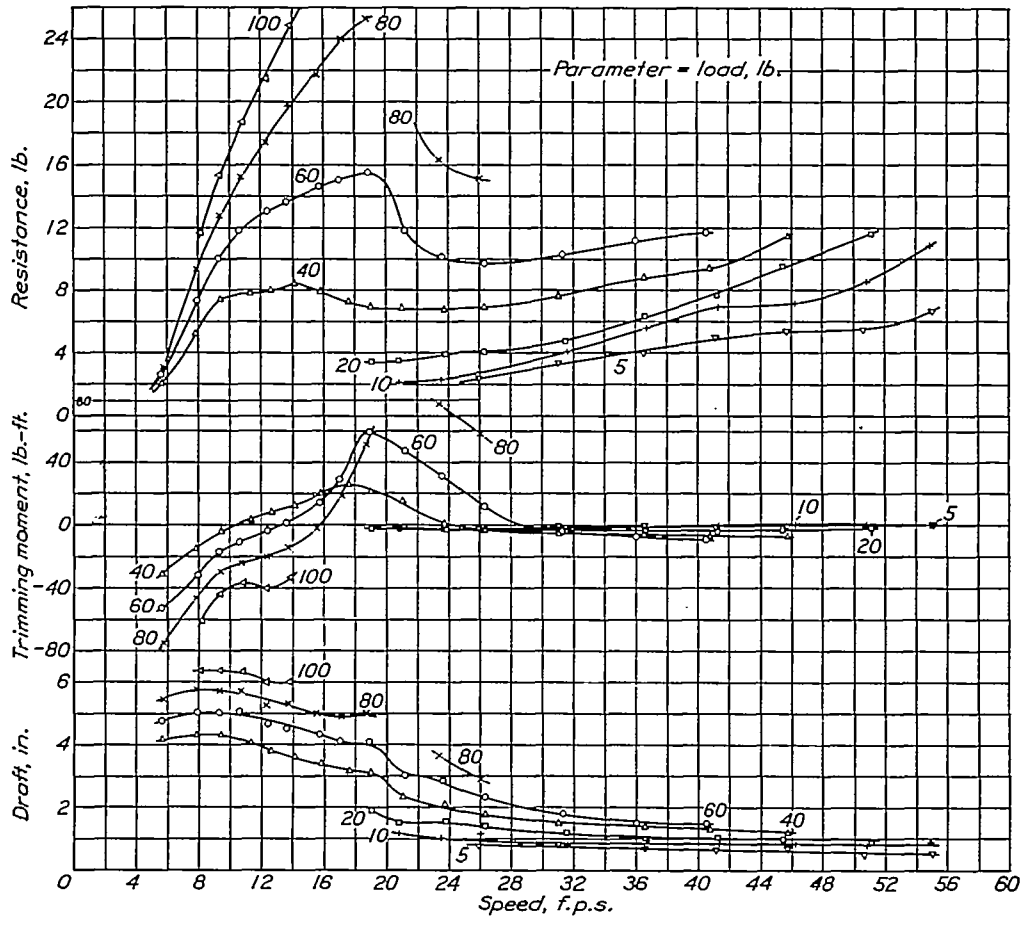

FIGURE 17.—Model 40-AE. Resistance, trimming moment, and draft. $\tau=5°$.

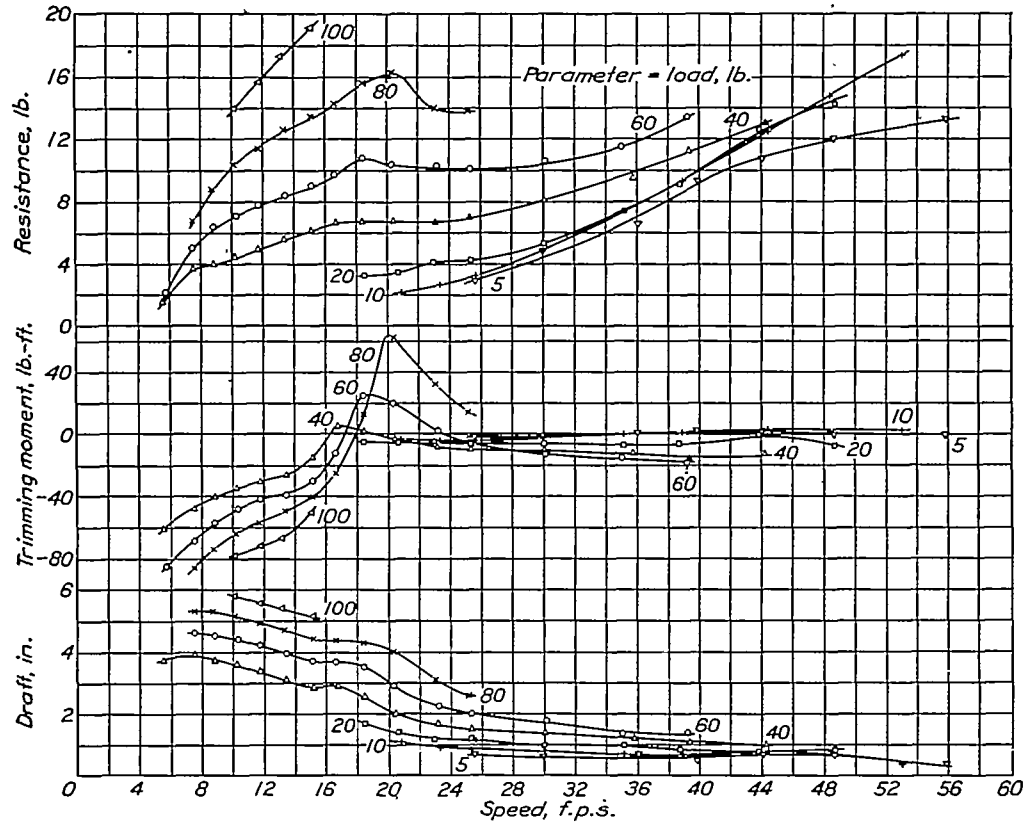

FIGURE 18.—Model 40-AE. Resistance, trimming moment, and draft. $\tau=7°$.

The resistance coefficient at zero moment and the angle for zero moment referred to a center of moments 4 inches ahead of the step on the model are plotted against speed in figures 58 to 67. Although these values were obtained from the free-to-trim tests in the tank, the values deduced from the data for the fixed-trim runs were found to check them closely. The characteristics at zero trimming moment or at an assumed thrust moment may be deduced for other positions of the center of gravity from suitable cross plots of figures 3 to 32.

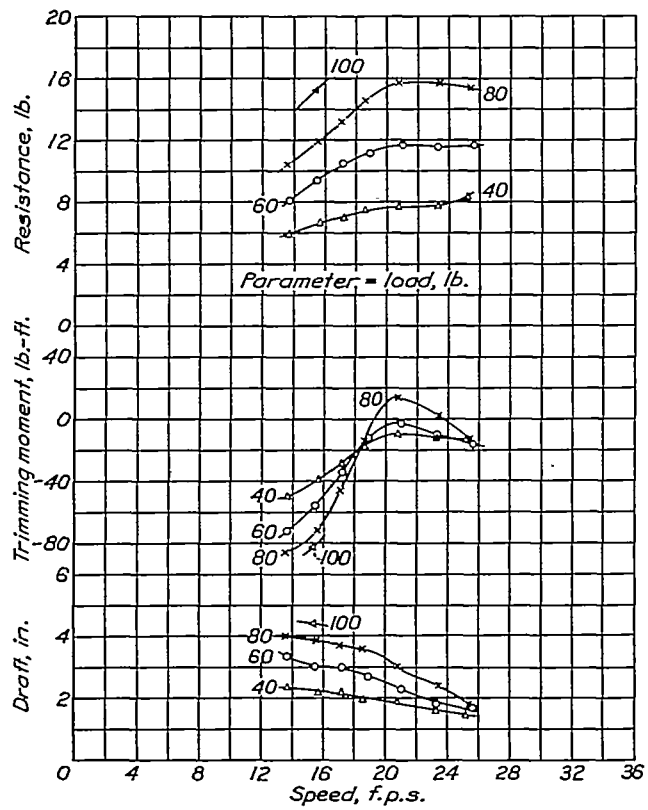

FIGURE 19.—Model 40-AE. Resistance, trimming moment, and draft. $\tau=9°$.

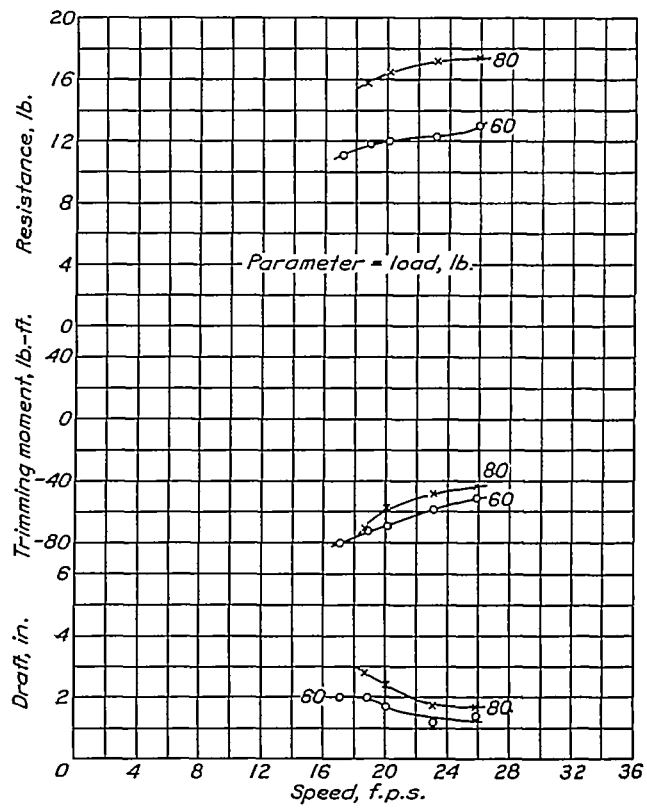

FIGURE 20.—Model 40-AE. Resistance, trimming moment, and draft. $\tau=11°$.

DISCUSSION OF RESULTS

BEST-ANGLE DATA

Comparisons of the characteristics of the hull forms may be made by cross-plotting the values of figures 38 to 57 against load coefficient at representative speed coefficients. Suitable cross curves for comparisons among the hulls are shown in figures 68, 69, and 71. The spray patterns may be compared by means of the photographs of figures 70 and 72.

Effect of form of forebody.—From figures 68 and 69 it is seen that the differences between the characteristics of the normal and developable forebodies are small for the smooth-water and fixed-trim conditions reproduced in the tank tests. The load-resistance ratios Δ/R for the developable form are slightly higher at the hump of the C_R curves and slightly lower at high planing speeds. When the developable forebody is used with the pointed afterbody, the maximum positive trimming-moment coefficient is slightly lower and the values at $C_V=7.0$ are larger in the negative direction. With the no-step afterbody, the maximum positive C_M is slightly lower at heavy loads and greater at light loads, whereas the high speed C_M values closely correspond. The differences in the best angle of trim are within the accuracy of determination.

Figure 70 shows the height and volume of spray thrown from the two types of forebodies to be practically identical for smooth-water operation. The water line does not extend far enough forward, however, to judge the action of the bow in rough water in the conditions shown. Apparently, the desirability of using the form of developable surface found on forebody B depends on its cleanness of running and the effect of the convex bow sections on resistance when driving through waves. An experimental determination of such qualities in the tank is difficult to carry out at the present time and is at best only an approximation of actual sea conditions.

Effect of form of afterbody.—The characteristics of the models consisting of the normal forebody and the various afterbodies are compared in figures 71 and 72. The Δ/R values with the pointed afterbody are lowest at the hump in the C_R curves and generally slightly higher at high planing speeds. With the no-step

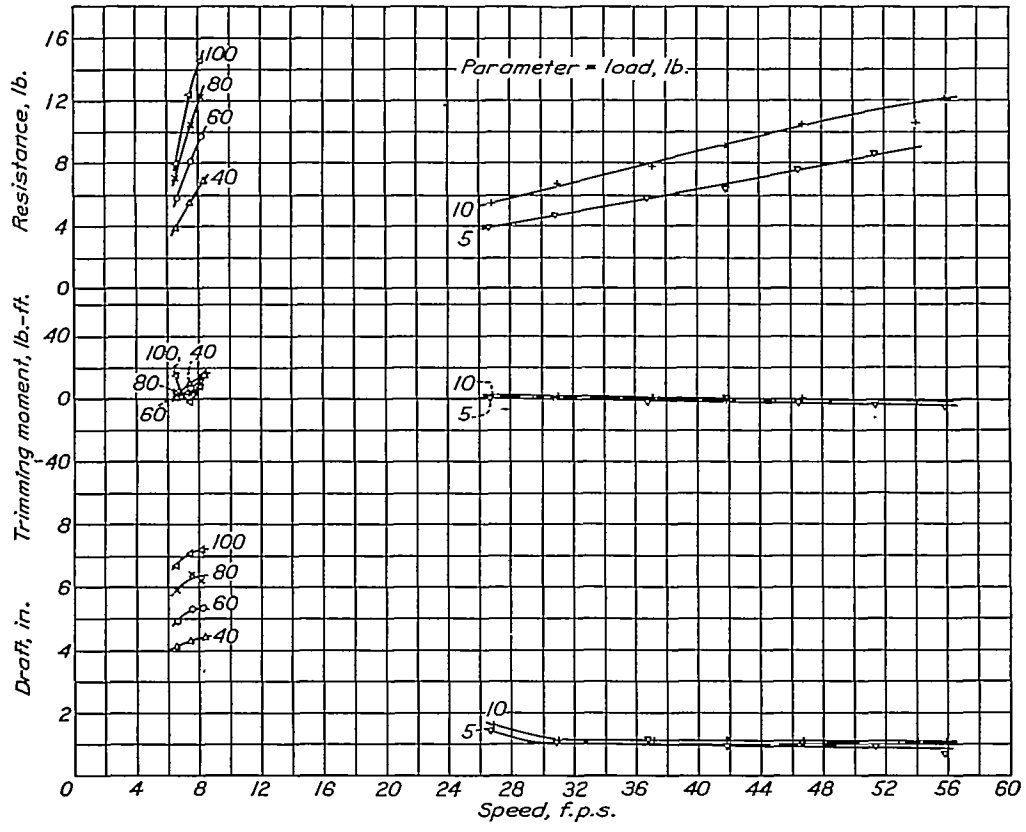

FIGURE 21.—Model 40-BC. Resistance, trimming moment, and draft. $\tau = 2°$.

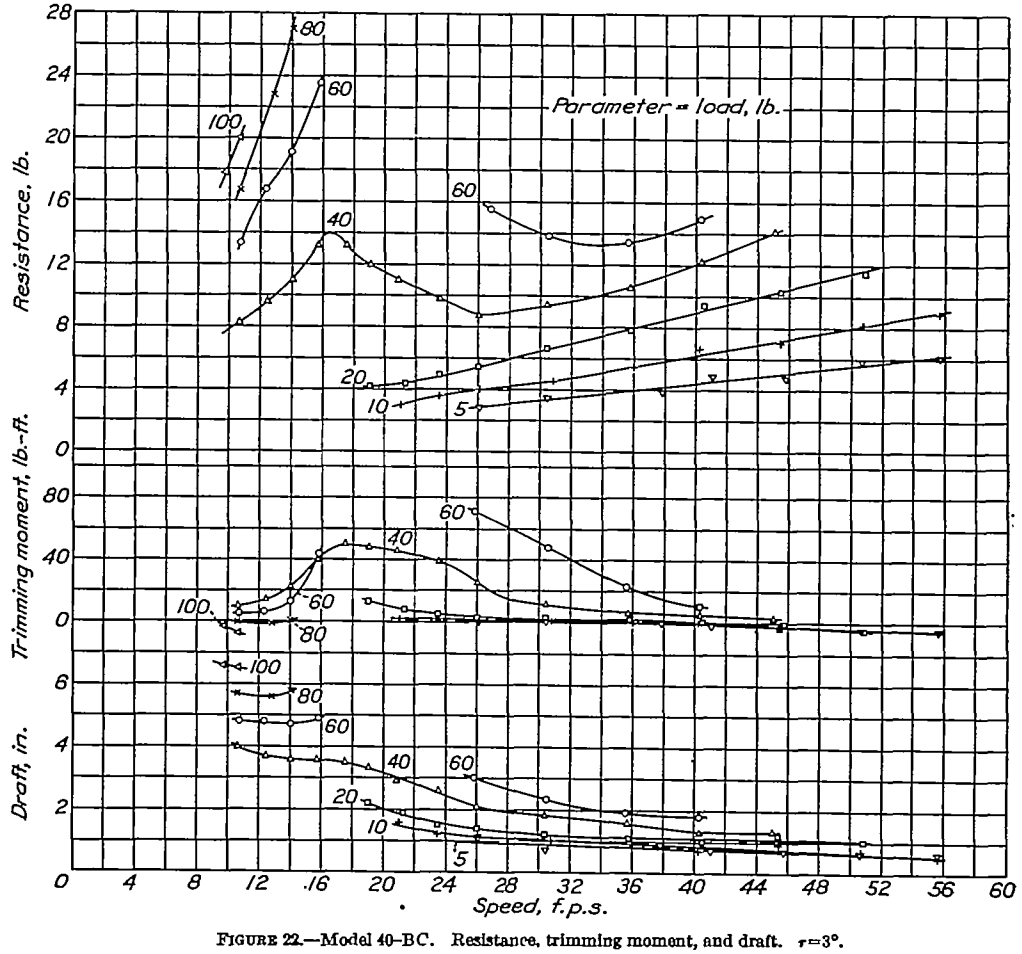

FIGURE 22.—Model 40-BC. Resistance, trimming moment, and draft. $\tau = 3°$.

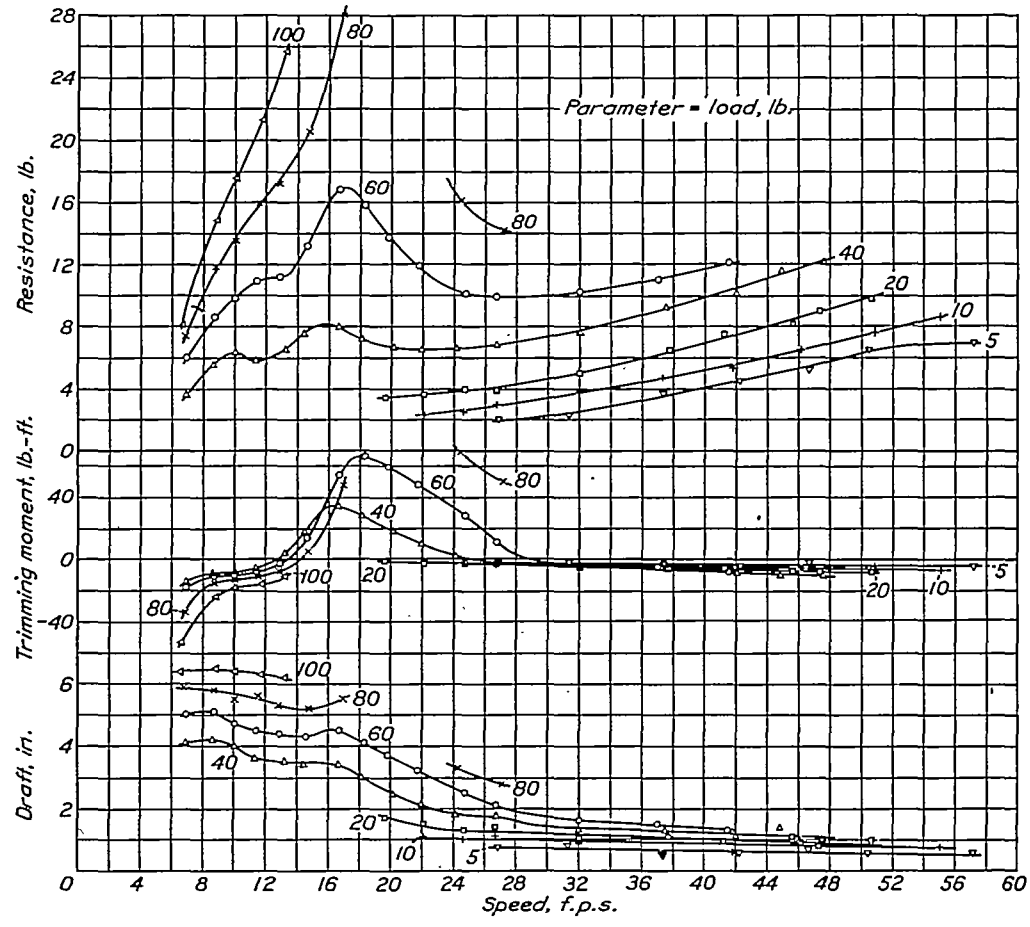

FIGURE 23. Model 40-BC. Resistance, trimming moment, and draft. $\tau = 5°$.

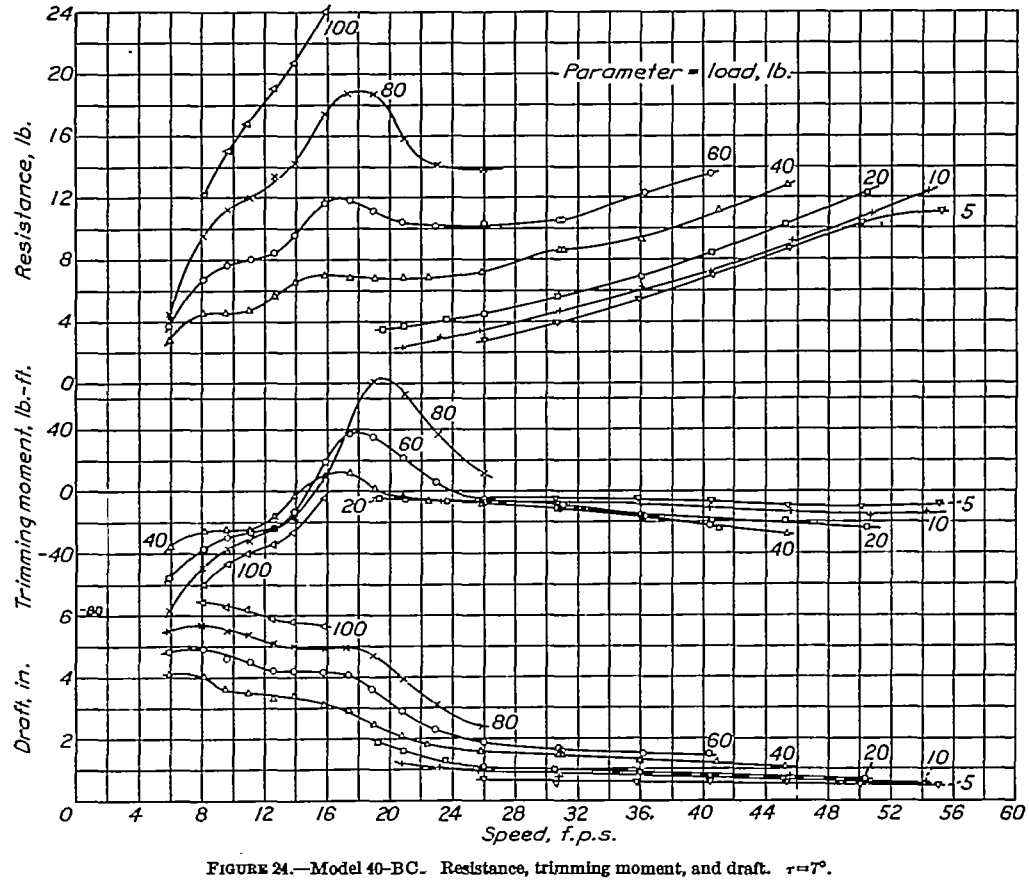

FIGURE 24.—Model 40-BC. Resistance, trimming moment, and draft. $\tau = 7°$.

afterbody the Δ/R values at the hump are slightly superior to those with the second-step afterbody; at medium planing speeds, inferior; and at high planing speeds, practically equal. The second-step afterbody gives the highest positive C_M and the no-step afterbody gives the lowest. There is little choice in trimming-moment characteristics at high speeds. The most favorable trim with the second-step afterbody is slightly lower near the hump speed. At high speeds, the best trim angle with all the afterbodies is practically the same.

The superiority of the performance with the second-step and no-step afterbodies at the best trim hump is attributed to the larger planing area provided by them when immersed at low speeds. The slight improvement given by the pointed afterbody at high speeds is probably because of the smaller area offered to the water coming from the forebody because the lift is produced chiefly by the main planing bottom forward of the step. From considerations of high-speed resistance, it appears desirable to carry the load on the forebody of a hull because the afterbody is operating in its wake and contributes a greater share of frictional resistance in proportion to the load it carries.

The photographs of figure 72 show the blisters coming from the forebody and also make it possible to get an idea of the action of the afterbody. The similarity of the secondary blisters coming from the after part of the model to those from the forebody indicates that at these speeds the afterbodies produce lift with the exception of the pointed afterbody, which seems to be clear at 19.7 feet per second. In general, the various models are fairly clean considering the heavy loads carried in proportion to their size.

FREE-TO-TRIM DATA

Figures 58 to 67 show the performance of the hulls at zero trimming moment around a center-of-gravity position 4 inches ahead of the step on the model. At low speeds and heavy loads some of the forms, particularly 40–BE, tend to remain below the best trim to such an extent that the resulting resistance peak is higher than what may be called the "real hump" corresponding to the maximum resistance at best trim angle. The negative thrust moment that usually exists would aggravate this condition. At speed coefficients corresponding to the real hump, however, the trim at zero moment is higher than the best trim so that the thrust moment would tend to lower the resistance. Any control moment available from the elevators in the slipstream at these low speeds can, of course, be used to favor the take-off. The performance before the hulls attain planing speeds is therefore dependent on the position of the center of gravity, the magnitude of the thrust moment, and the amount of control that the pilot can bring into play to maintain the best trim angle.

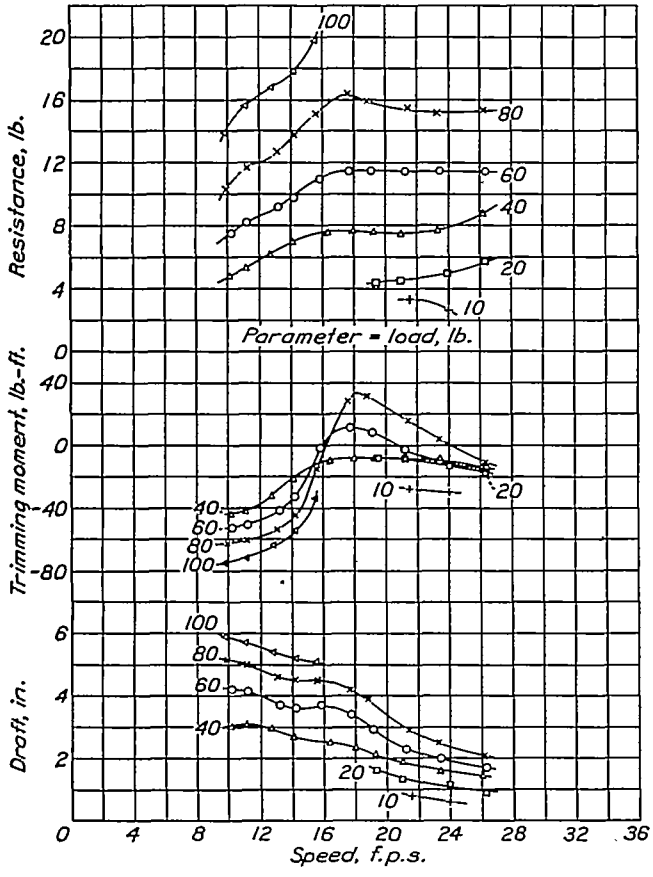

FIGURE 25.—Model 40-BC. Resistance, trimming moment, and draft. $\tau=9°$.

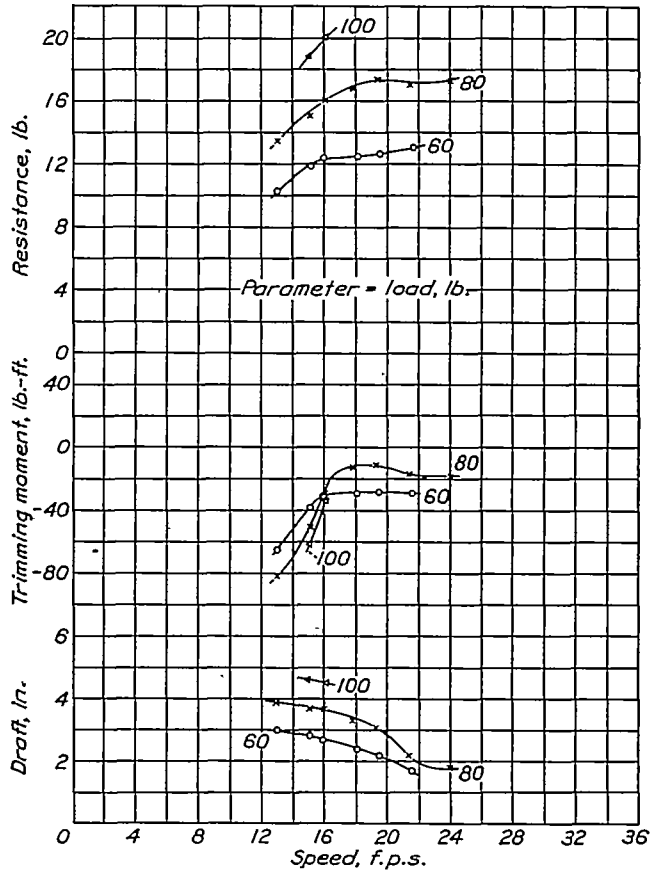

FIGURE 26.—Model 40-BC. Resistance, trimming moment, and draft. $\tau=11°$.

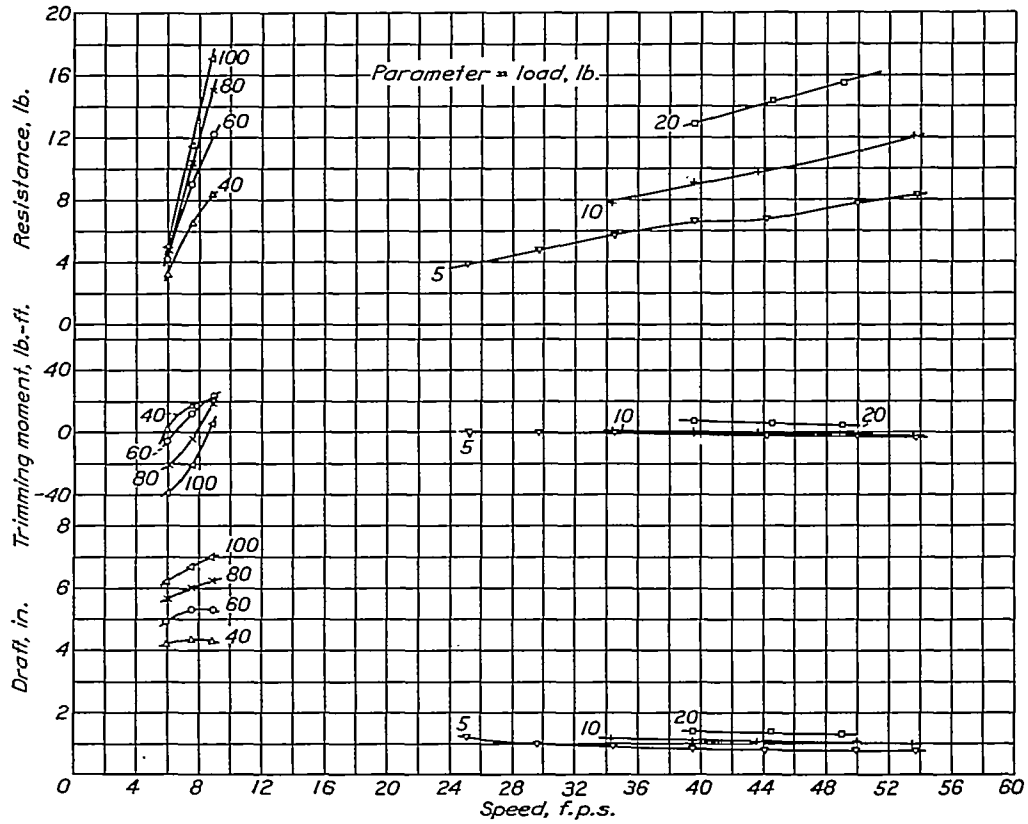

FIGURE 27.—Model 40-BE. Resistance, trimming moment, and draft. $\tau=2°$.

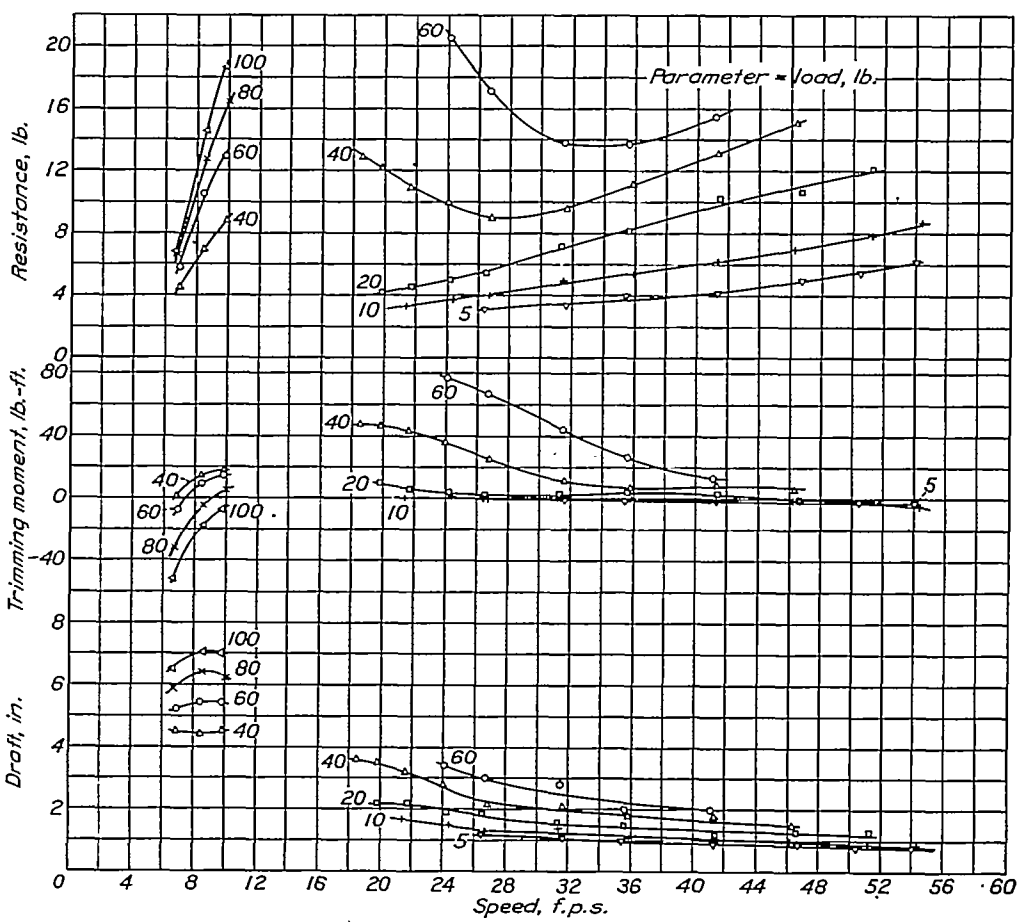

FIGURE 28.—Model 40-BE. Resistance, trimming moment, and draft. $\tau=3°$.

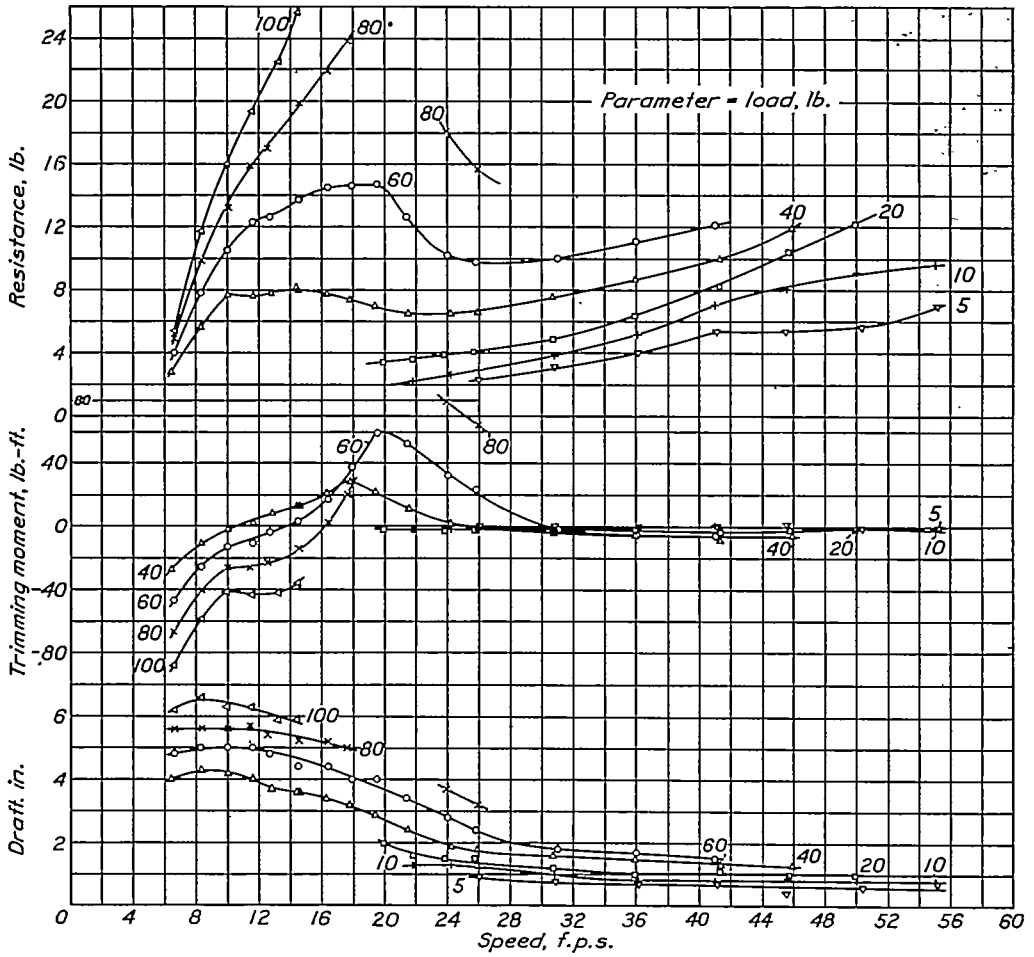

FIGURE 29.—Model 40-BE. Resistance, trimming moment, and draft. $\tau=5°$.

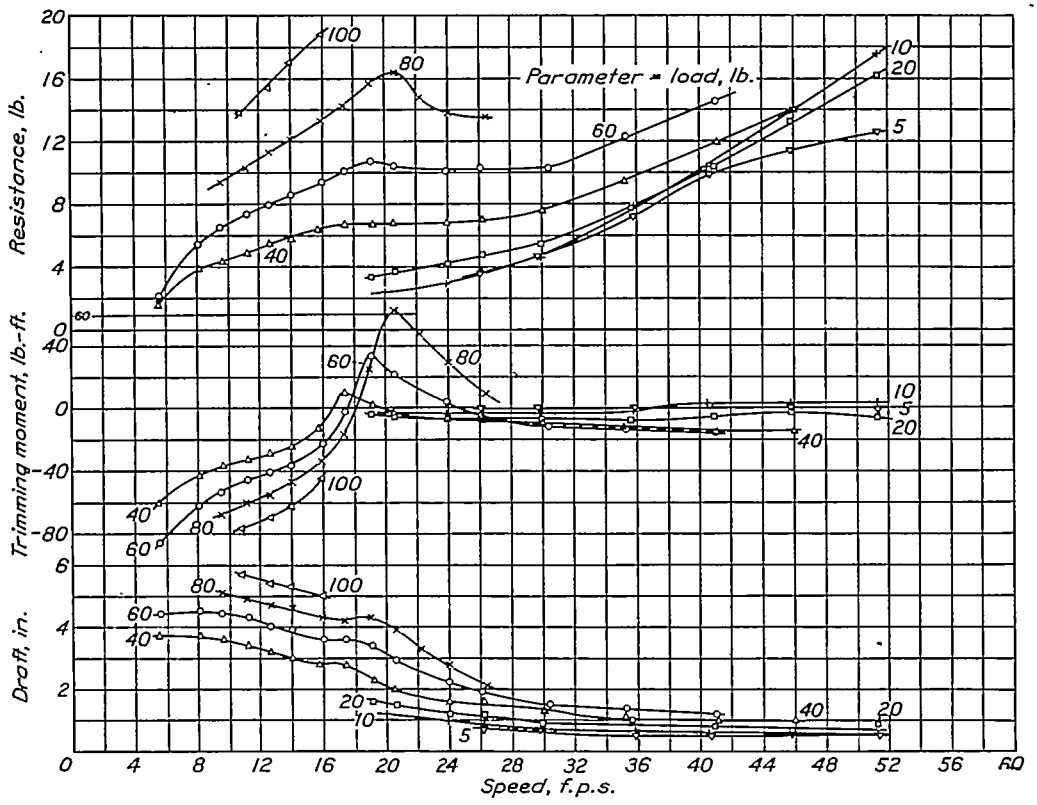

FIGURE 30.—Model 40-BE. Resistance, trimming moment, and draft. $\tau=7°$.

TAKE-OFF EXAMPLES

The application of the data obtained from these models is illustrated by the following examples:

Example 1.—A hypothetical flying boat or amphibian suitable for cargo or passenger service is represented by the following assumed data:

Gross load, lb	8,000
Wing area, sq. ft	550
Horsepower	600
Effective aspect ratio including ground effect	10
Parasite-drag coefficient excluding hull	0.03
Airfoil section	Clark Y

Model 40–BC is selected as the hull and a maximum beam of 5.2 feet is used. This beam will give a moderately high beam loading at the hump (C_Δ=about 0.75) where about 85 percent of the gross weight will be on the water. The best angle of wing setting is found by the method of reference 3 to be about 5°. The center of gravity of the complete boat is taken to be the same as that used in the free-to-trim tests on these models and it is arbitrarily assumed that the craft will run free to trim to a speed coefficient of 2.4 and at best trim angle at higher speeds. The water resistance plus air drag ($R+D$) is computed by the method of reference 3 using the free-to-trim curves up to C_V=2.4. The resultant curve is plotted in figure 73 together with the thrust obtained from the curves of reference 4. From this figure it may be seen that there is considerably more excess thrust at the hump than at the second critical point near get-away. A somewhat smaller hull should then give a little better take-off performance. The take-off time and distance are determined from the $1/a$ and V/a curves, respectively, both of which are plotted in figure 73 (b). The time is found to be 24.2 seconds and the length of run 1,480 feet.

The trim-angle curve for this take-off is plotted in figure 74 (a) and the trimming moments to obtain these trim angles are plotted in figure 74 (b). This trimming-moment-curve was obtained from figure 56 and was corrected for the difference between the center of gravity chosen and the center of moments used in the fixed-trim tests. If the center of gravity chosen had been other than that used for the free-to-trim tests it would have been necessary to compute the free-to-trim resistance from the test results given in figures 21 to 26.

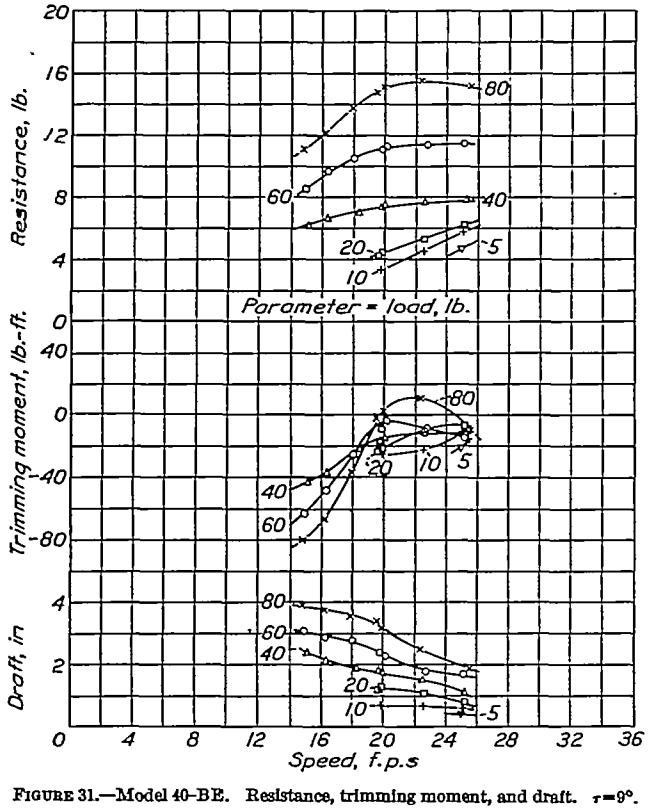

FIGURE 31.—Model 40-BE. Resistance, trimming moment, and draft. τ=9°.

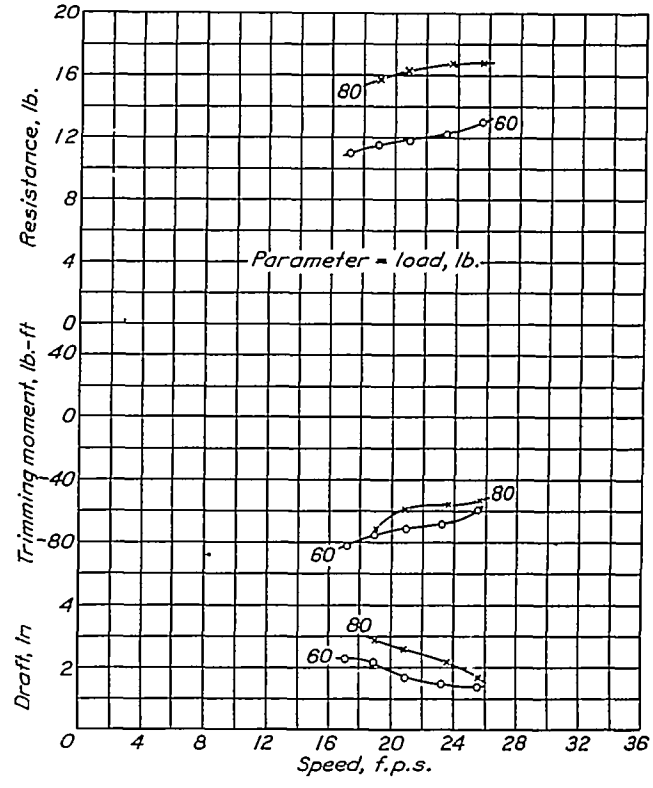

FIGURE 32.—Model 40-BE. Resistance, trimming moment, and draft. τ=11°.

In practice, if the free-to-trim calculations indicate that there is a reasonable amount of excess thrust at low speeds, the free-to-trim resistance may be used in the calculations for take-off time and distance without appreciable error. If, however, it appears desirable and the design is sufficiently advanced to determine the aerodynamic moments, the minimum resistance obtainable may be calculated from the test data.

Example 2.—A hypothetical small low-powered flying boat will be considered. This craft is presumably to be built at a reasonable cost without a great number

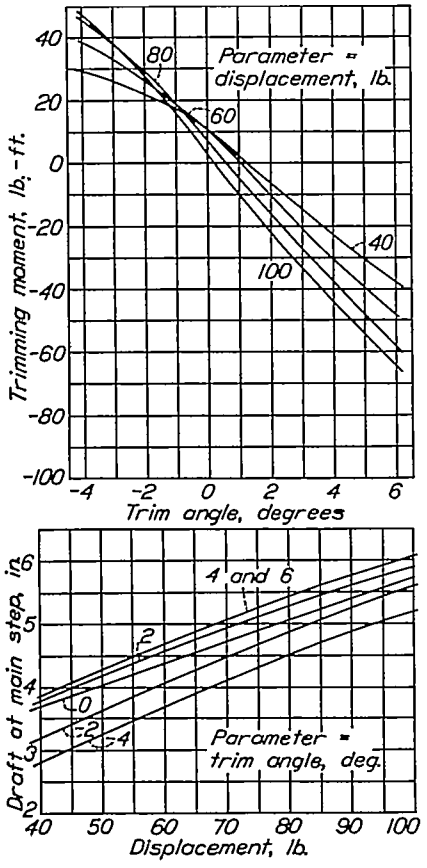

FIGURE 33.—Model 40-AC. Trimming moments and drafts at rest.

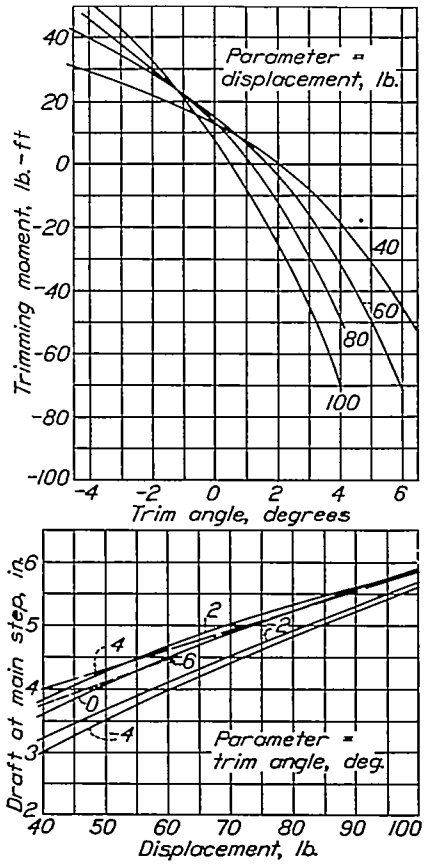

FIGURE 34.—Model 40-AD. Trimming moments and drafts at rest.

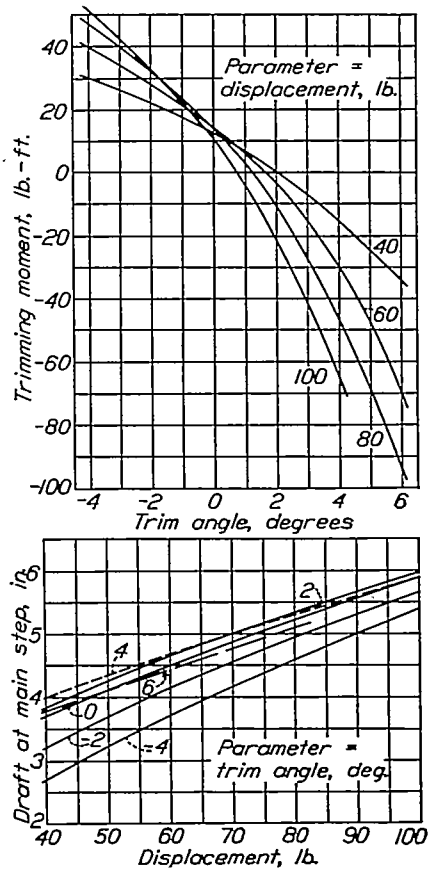

FIGURE 35.—Model 40-AE. Trimming moments and drafts at rest.

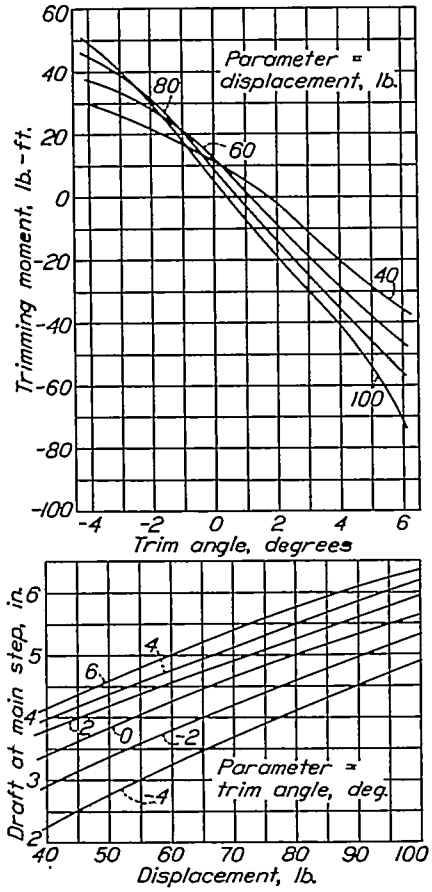

FIGURE 36.—Model 40-BC. Trimming moments and drafts at rest.

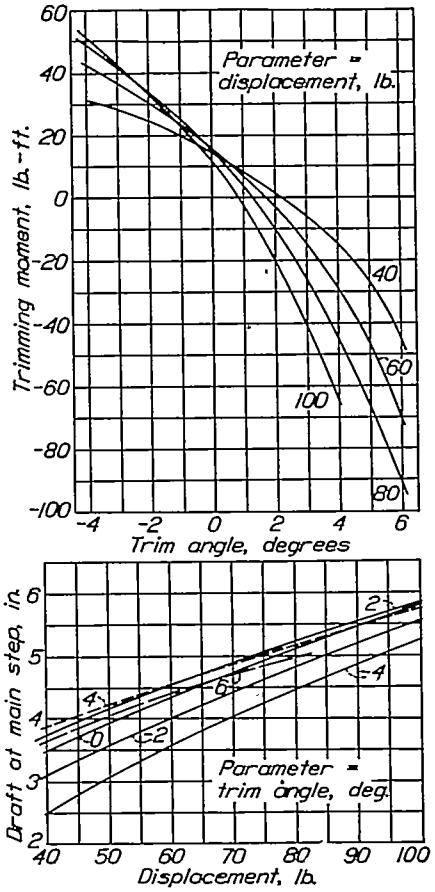

FIGURE 37.—Model 40-BE. Trimming moments and drafts at rest.

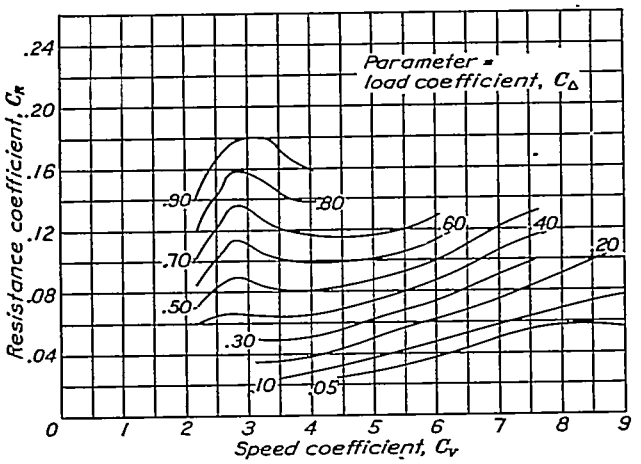

FIGURE 38.—Model 40-AC. Variation of resistance coefficient at best trim angle with speed coefficient.

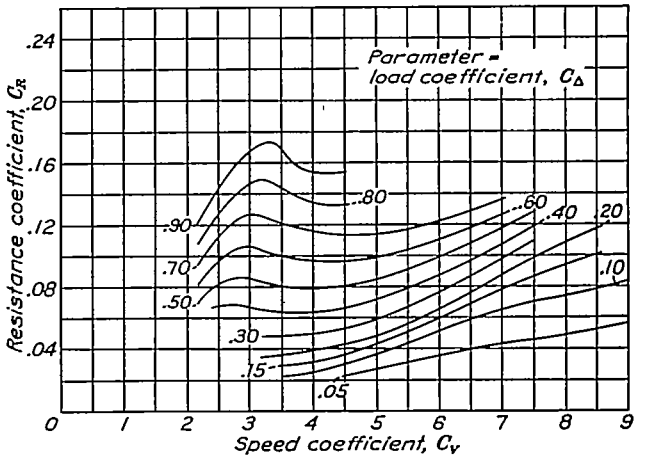

FIGURE 39.—Model 40-AD. Variation of resistance coefficient at best trim angle with speed coefficient.

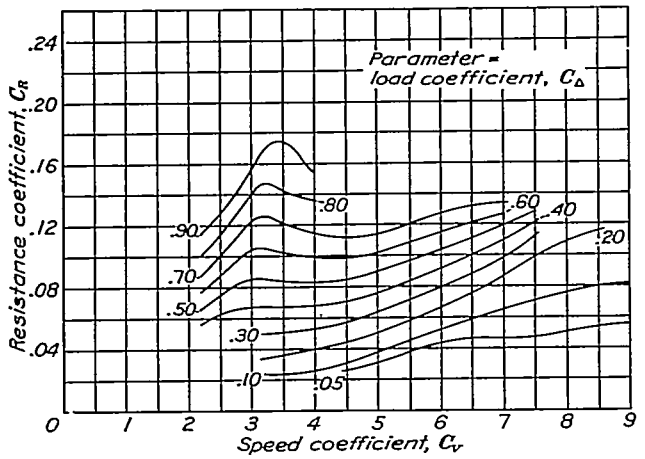

FIGURE 40.—Model 40-AE. Variation of resistance coefficient at best trim angle with speed coefficient.

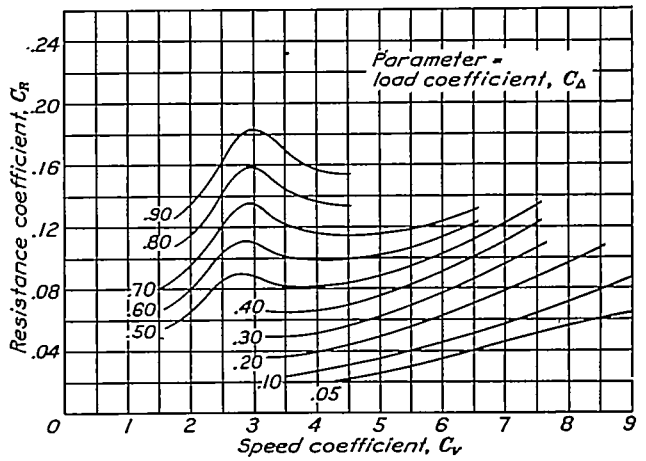

FIGURE 41.—Model 40-BC. Variation of resistance coefficient at best trim angle with speed coefficient.

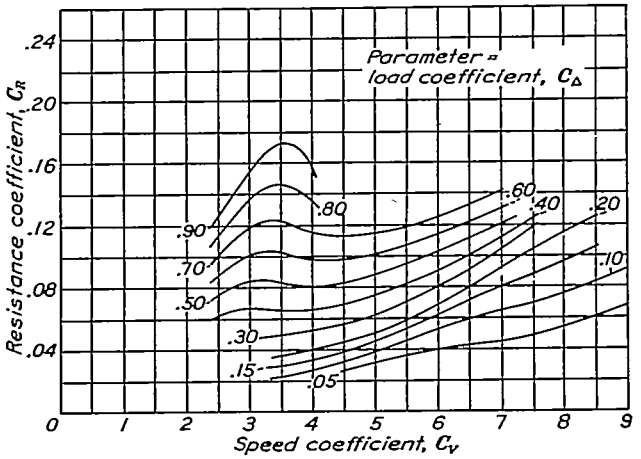

FIGURE 42.—Model 40-BE. Variation of resistance coefficient at best trim angle with speed coefficient.

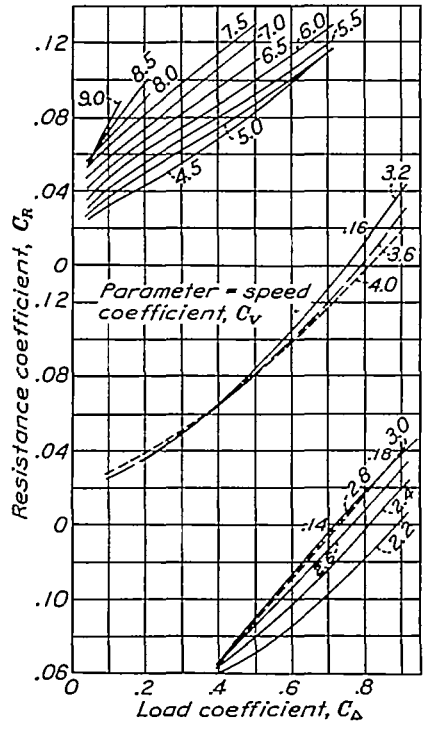

FIGURE 43.—Model 40-AC. Variation of resistance coefficient at best trim angle with load coefficient.

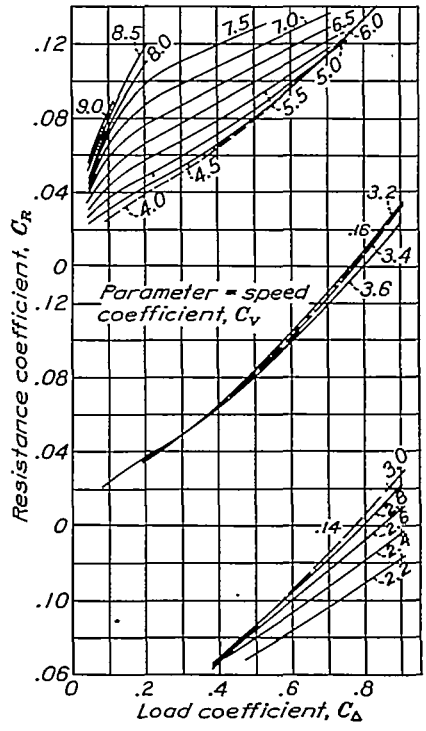

FIGURE 44.—Model 40-AD. Variation of resistance coefficient at best trim angle with load coefficient.

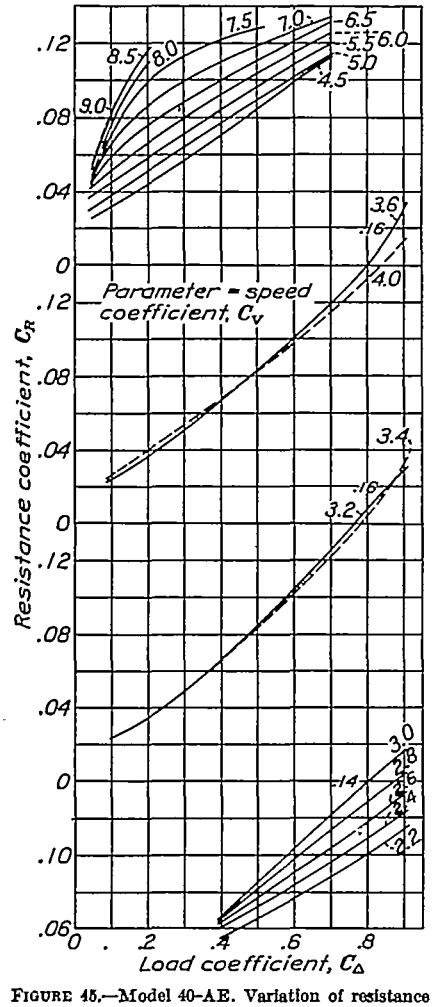

FIGURE 45.—Model 40-AE. Variation of resistance coefficient at best trim angle with load coefficient.

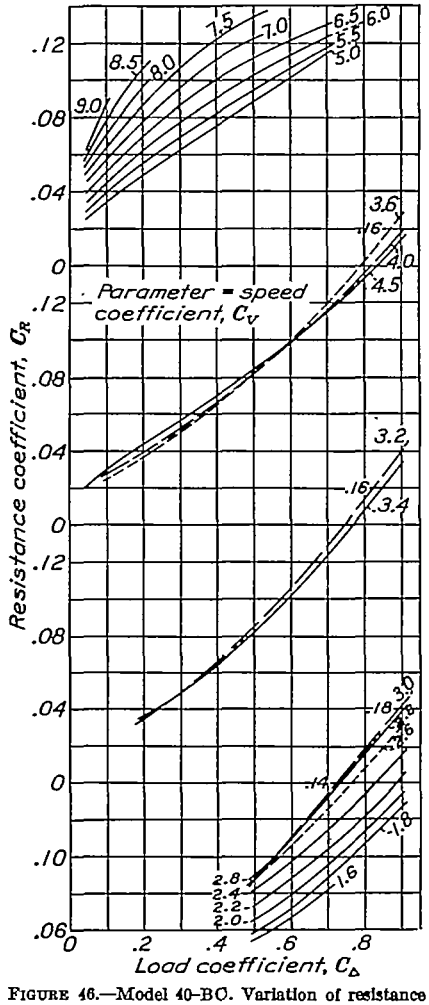

FIGURE 46.—Model 40-BC. Variation of resistance coefficient at best trim angle with load coefficient.

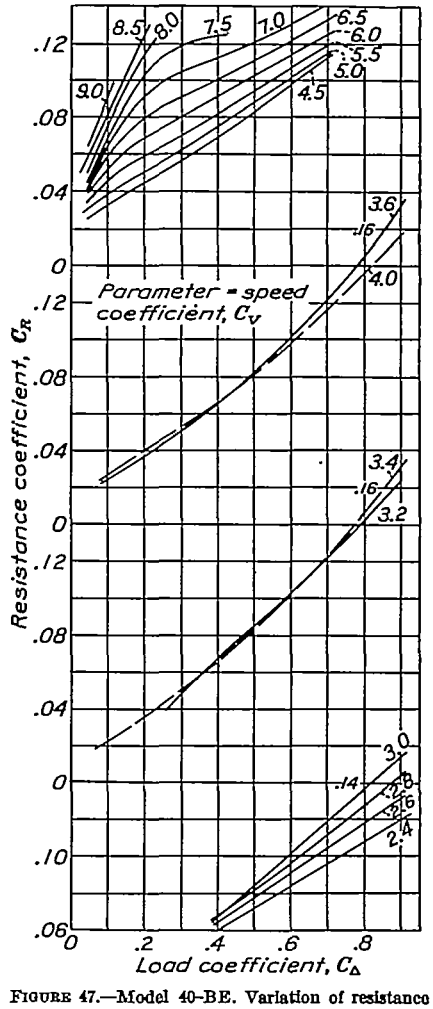

FIGURE 47.—Model 40-BE. Variation of resistance coefficient at best trim angle with load coefficient.

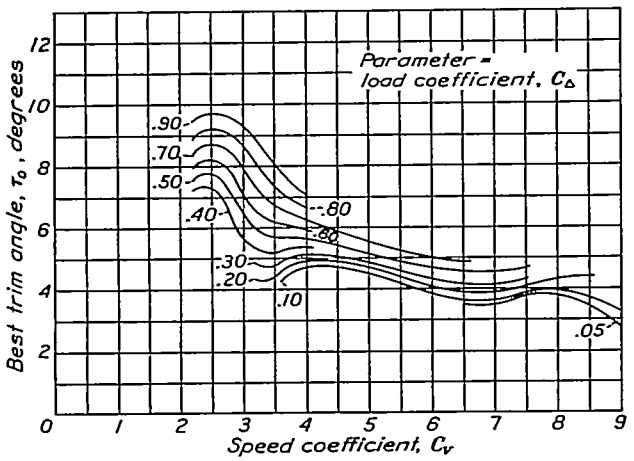

FIGURE 48.—Model 40-AC. Variation of best trim angle with speed coefficient.

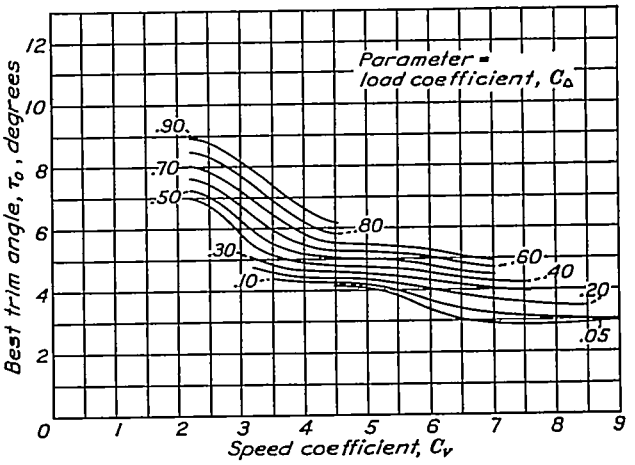

FIGURE 49.—Model 40-AD. Variation of best trim angle with speed coefficient.

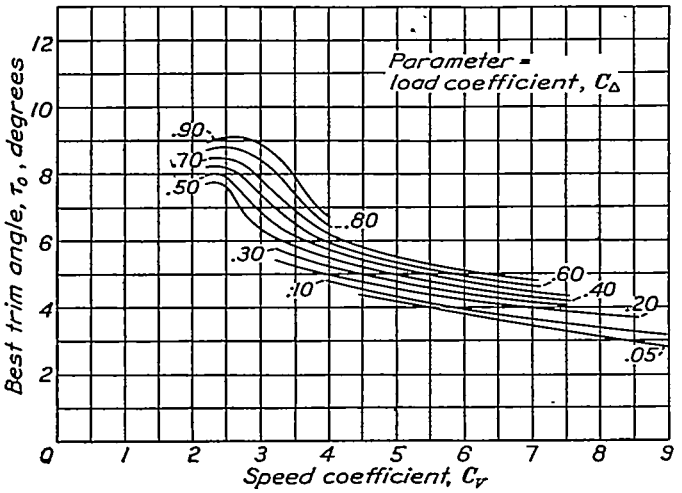

FIGURE 50.—Model 40-AE. Variation of best trim angle with speed coefficient.

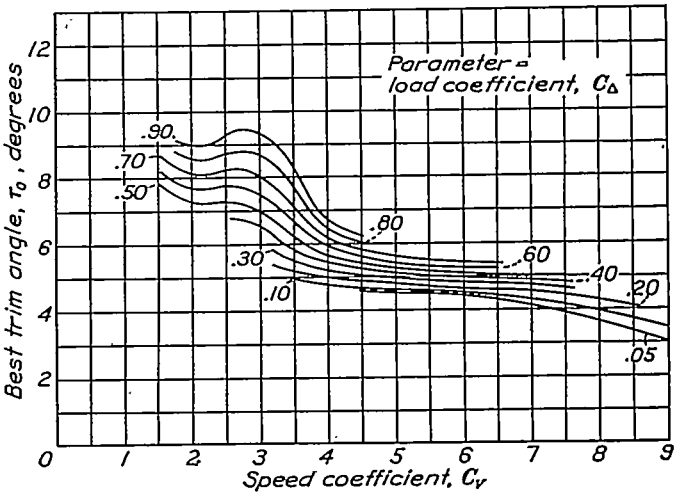

FIGURE 51.—Model 40-BC. Variation of best trim angle with speed coefficient.

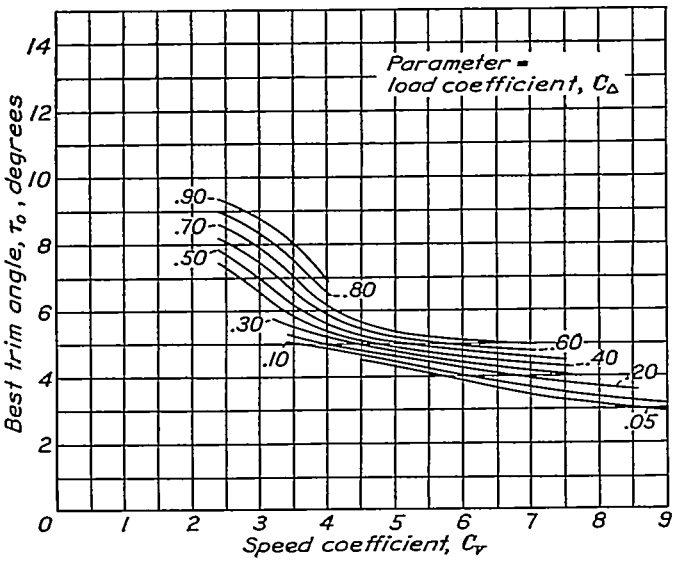

FIGURE 52.—Model 40-BE. Variation of best trim angle with speed coefficient.

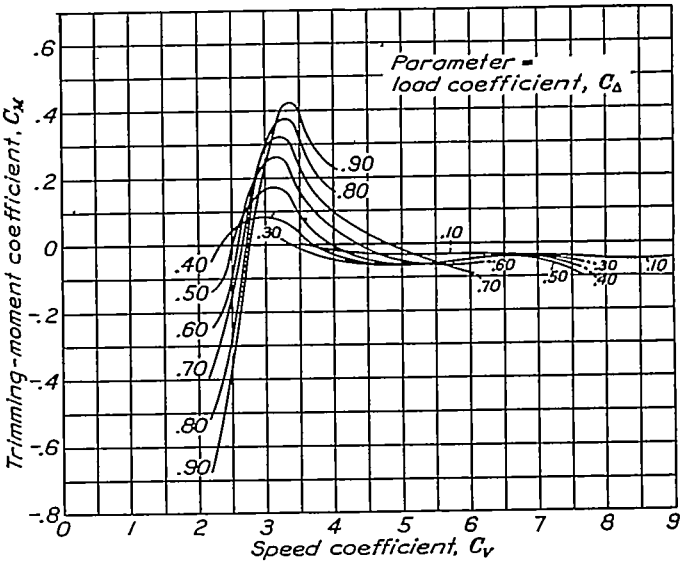

FIGURE 53.—Model 40-AC. Variation of trimming-moment coefficient at best trim angle with speed coefficient.

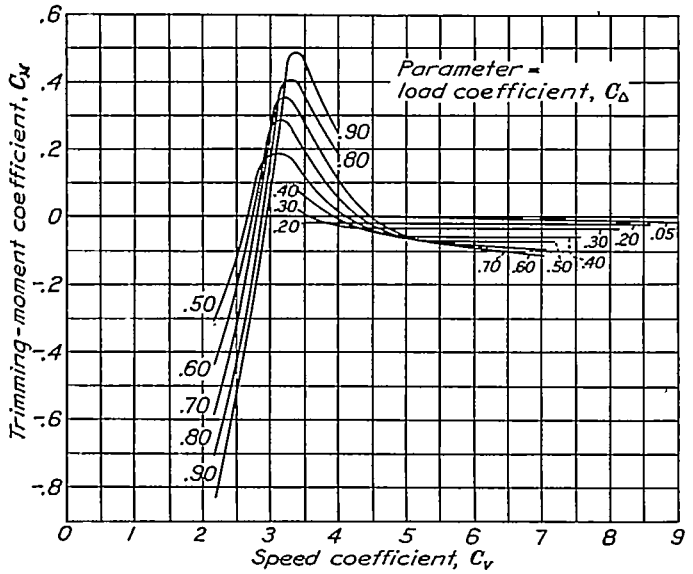

FIGURE 54.—Model 40-AD. Variation of trimming-moment coefficient at best trim angle with speed coefficient.

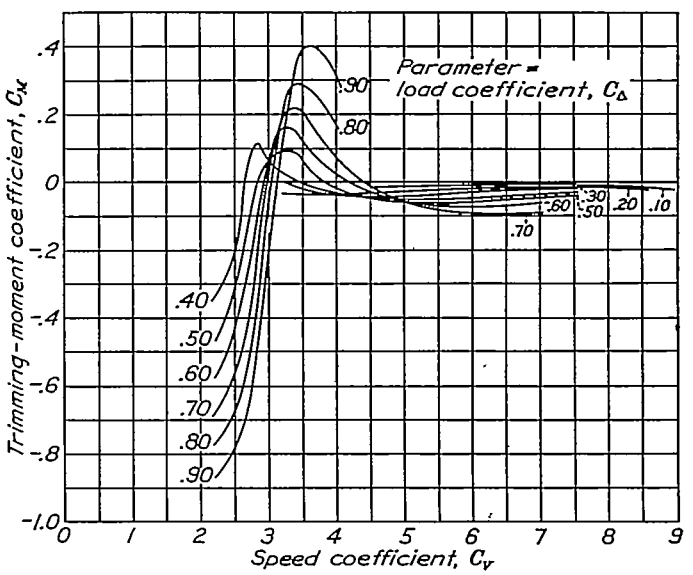

FIGURE 55.—Model 40-AE. Variation of trimming-moment coefficient at best trim angle with speed coefficient.

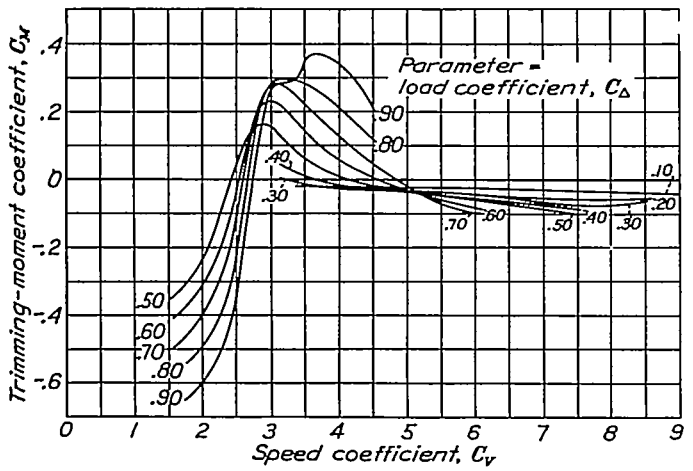

FIGURE 56.—Model 40-BC. Variation of trimming-moment coefficient at best trim angle with speed coefficient.

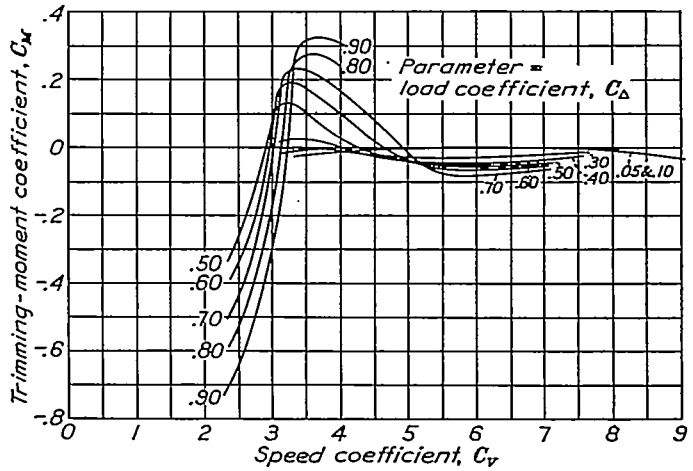

FIGURE 57.—Model 40-BE. Variation of trimming-moment coefficient at best trim angle with speed coefficient.

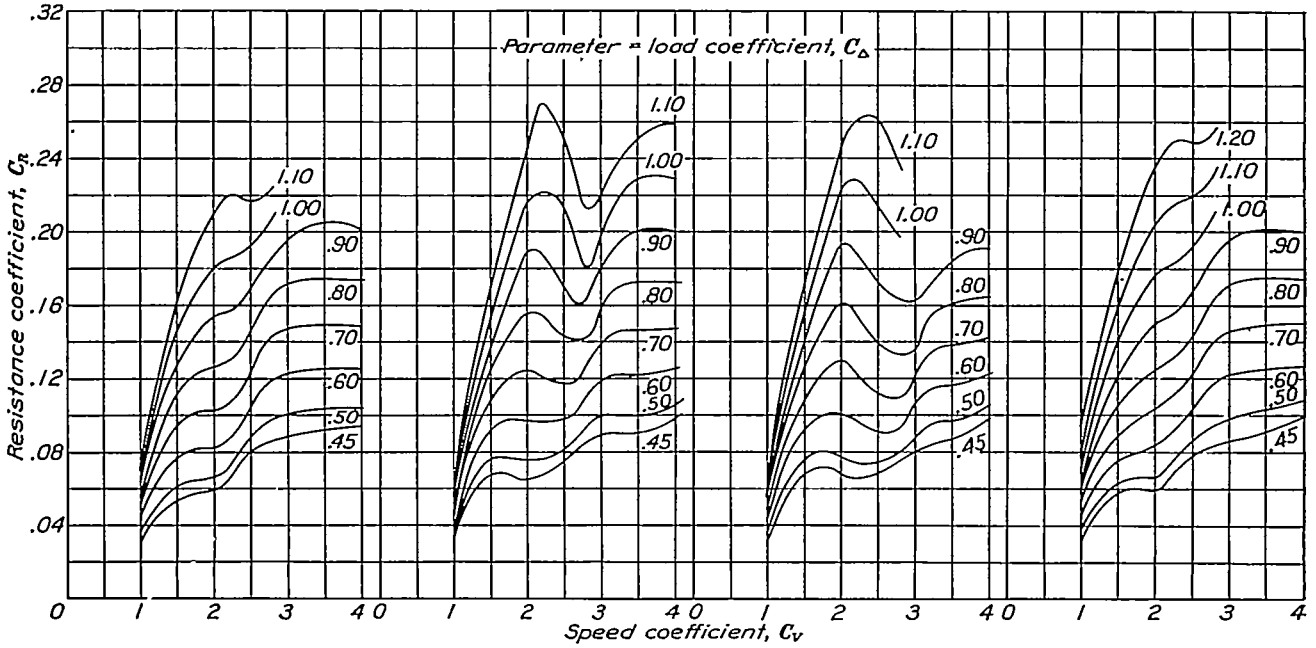

FIGURE 58.—Model 40-AC. FIGURE 59.—Model 40-AD. FIGURE 60.—Model 40-AE. FIGURE 61.—Model 40-BC.

Variation of resistance coefficient at zero trimming moment with speed coefficient. Free-to-trim tests.

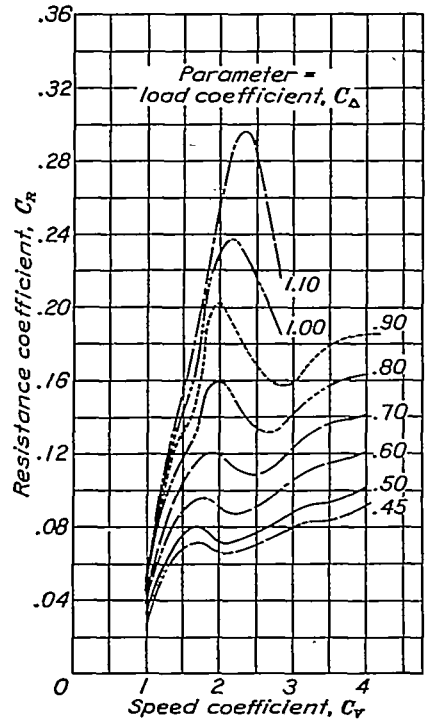

FIGURE 62.—Model 40-BE. Variation of resistance coefficient at zero trimming moment with speed coefficient. Free-to-trim tests.

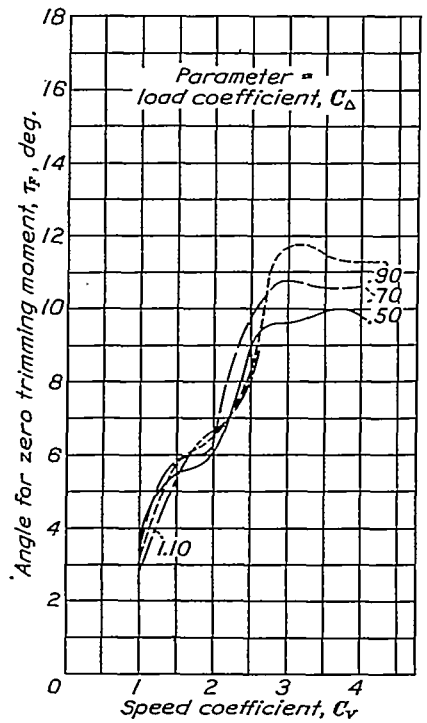

FIGURE 63.—Model 40-AC. Variation of trim angle for zero trimming moment with speed coefficient. Free-to-trim tests.

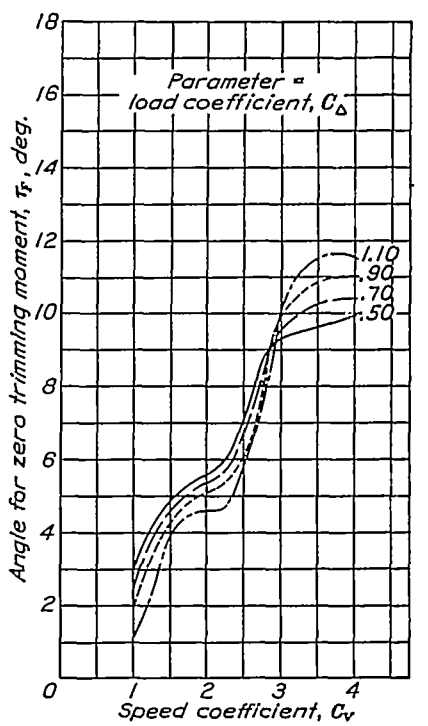

FIGURE 64.—Model 40-AD. Variation of trim angle for zero trimming moment with speed coefficient. Free-to-trim tests.

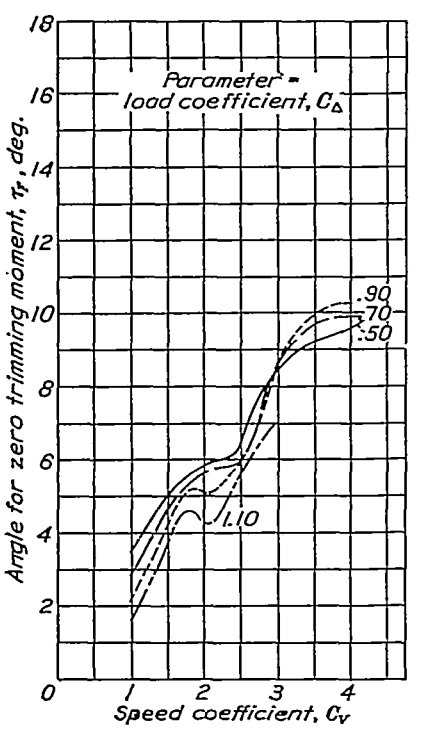

FIGURE 65.—Model 40-AE. Variation of trim angle for zero trimming moment with speed coefficient. Free-to-trim tests.

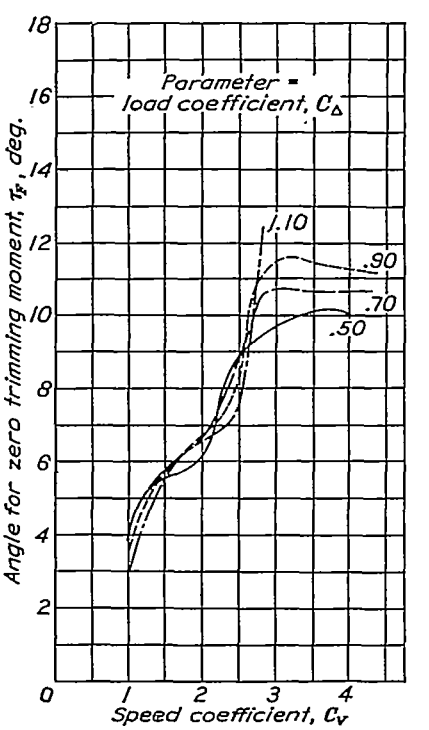

FIGURE 66.—Model 40-BC. Variation of trim angle for zero trimming moment with speed coefficient. Free-to-trim tests.

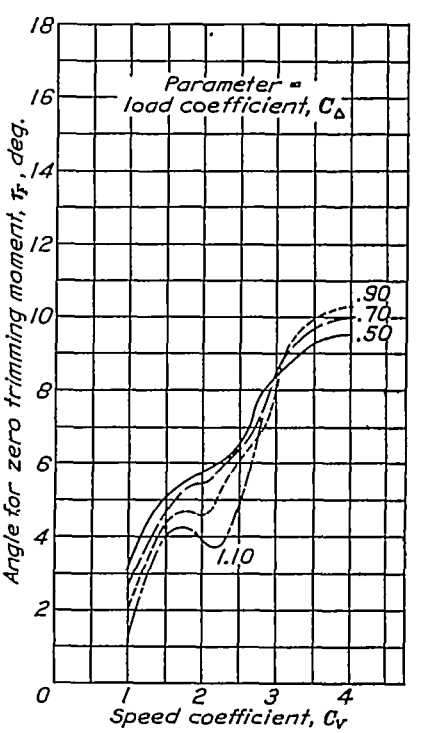

FIGURE 67.—Model 40-BE. Variation of trim angle for zero trimming moment with speed coefficient. Free-to-trim tests.

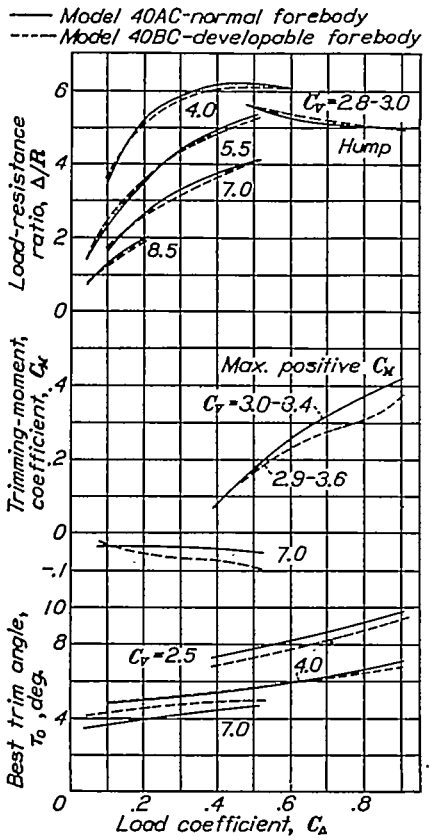

FIGURE 68.—Effect of developable forebody surface on characteristics at best trim angle. Pointed afterbody.

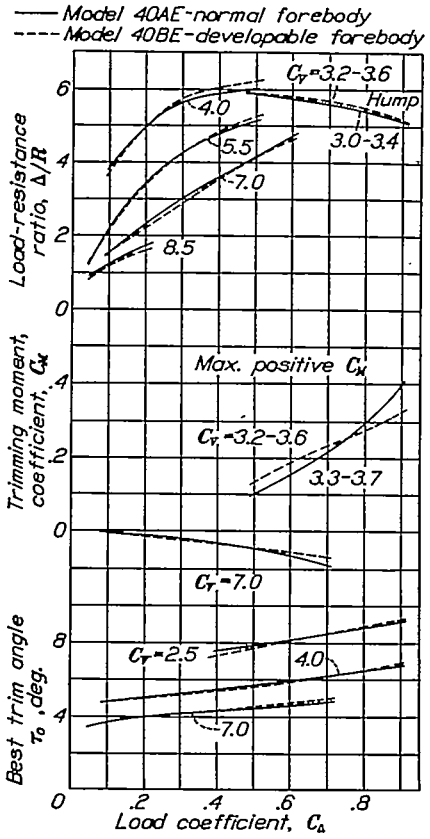

FIGURE 69.—Effect of developable forebody surface on characteristics at best trim angle. No-step afterbody.

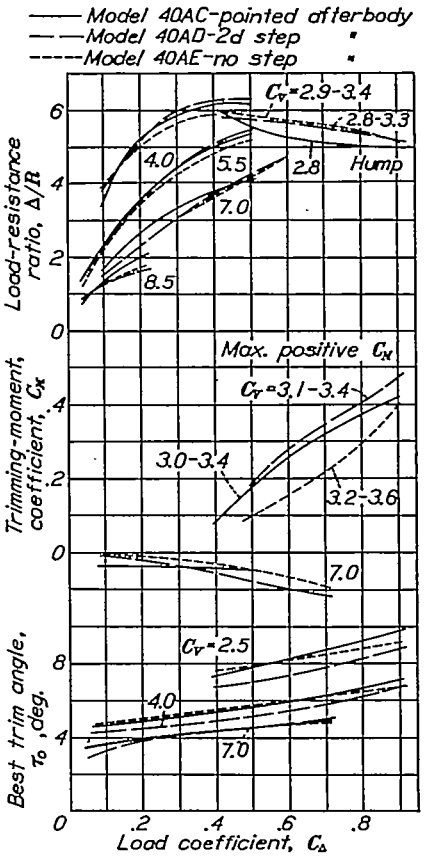

FIGURE 71.—Effect of afterbody form on characteristics at best trim angles. Normal forebody.

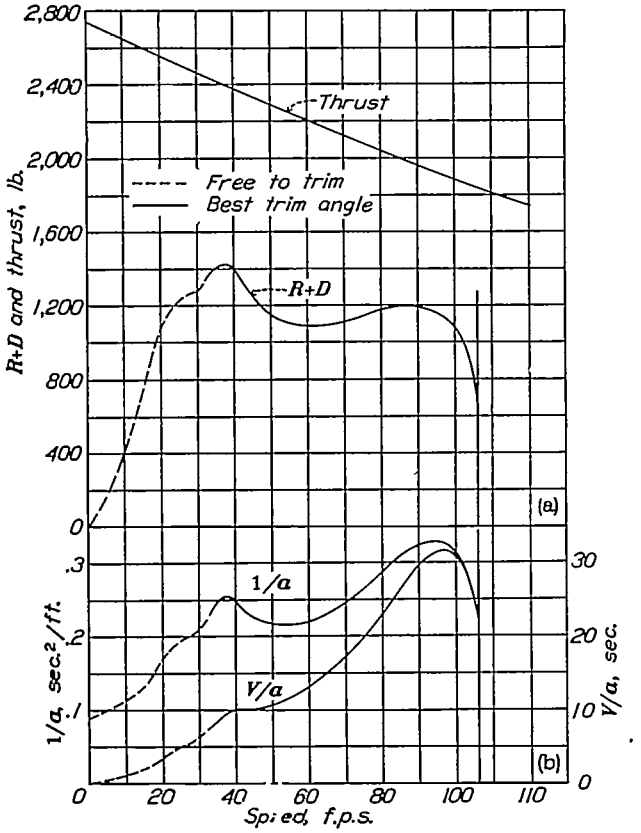

FIGURE 73.—Curves for determining take-off time and run for the 8,000-pound example.

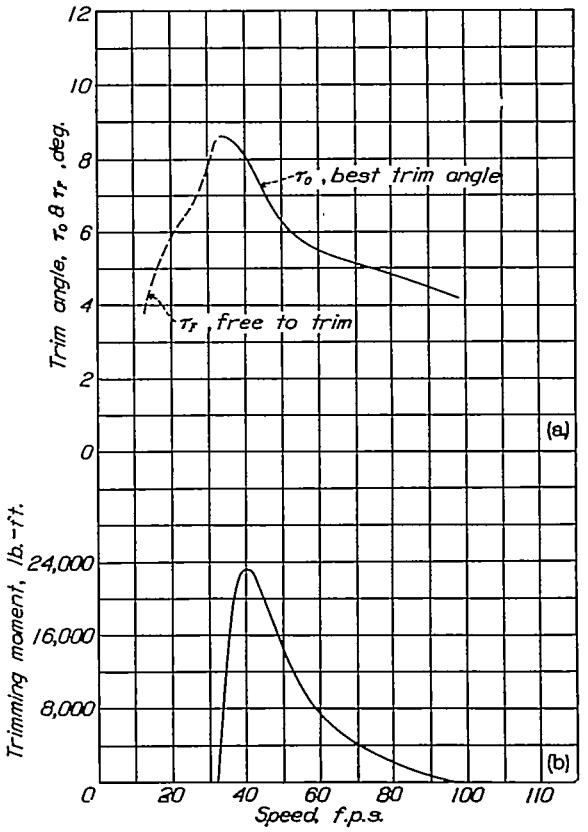

FIGURE 74.—Trim angle and trimming moment for the 8,000 pound example.

of refinements. The parasite drag is purposely assumed to be quite high. The following data are assumed:

Gross load, lb	2,000
Wing area, sq. ft	200
Horsepower	110
Effective aspect ratio including ground effect	10
Parasite-drag coefficient excluding hull	0.05
Airfoil section	Clark Y

best-angle total resistance at the hump. If sufficient controlling moment to increase the trim angles is available at low speeds, the low-speed resistance can be reduced. Examination of the $1/a$ and V/a curves shows, however, that this early resistance peak increases the take-off time less than 1 second and that the effect on the take-off distance is almost negligible. In fact, the excess thrust is found to be smallest at the

13.4 f. p. s.; τ=7°; Δ=40 lb.

14.0 f. p. s.; τ=7°; Δ=40 lb.

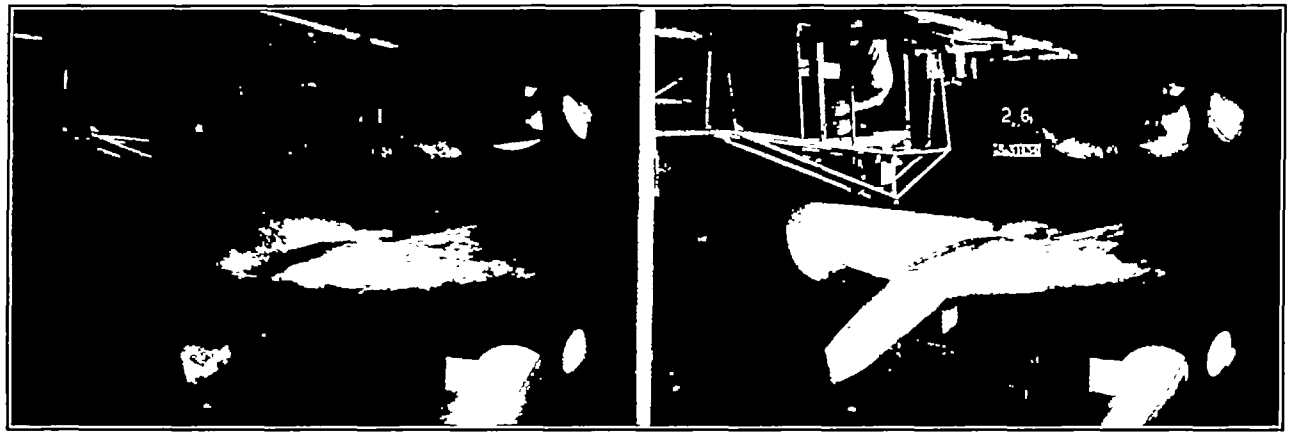

13.6 f. p. s.; τ=9°; Δ=80 lb.
Model 40AE, normal forebody.

14.8 f. p. s.; τ=9°; Δ=80 lb.
Model 40BE, developable forebody.

FIGURE 70.—Effect of developable forebody surface on spray pattern. No-step afterbody.

Model 40–BE is chosen for the hull and a maximum beam of 3.15 feet is used to give the maximum hull loading that can be used without extrapolating some of the curves. The angle of wing setting used is 4°. Again, the center of gravity is conveniently taken to be the same as that used in the free-to-trim tests of the hull.

Thrust, $R+D$, $1/a$, and V/a are plotted in figure 75. Trim angle and trimming moment are plotted in figure 76. The take-off time and distance are computed using the free-to-trim resistance curve to the point where it meets the best-angle resistance curve. The take-off time is 23.7 seconds and the length of run 1,300 feet.

It is seen that the free-to-trim total resistance ($R+D$) at low speeds is considerably greater than the critical point near get-away. It would seem from this fact that a smaller hull would give a substantial improvement in water performance but the loading used here appears to be very close to the practical limit. Any further increase of the load coefficient would probably result in too much spray at low speeds. Some improvement could be obtained by a higher wing setting as the high-speed hump occurs very near the stalling speed, but the improvement in take-off performance would probably be gained at the cost of a poorer flying attitude. Furthermore, if the angle of wing setting is increased too much, the problem may be complicated by the stalling of the wing at the high trim angles required near the hump.

If the trimming moment required to obtain best trim angle at the hump (fig. 76(b)) is found to be

excessive, an angle somewhere between the best angle and the zero trimming-moment angle can probably be obtained that will increase the hump only slightly, as indicated by the comparatively small difference between the minimum $R+D$ and the free-to-trim $R+D$ at a speed of 38 feet per second (fig. 75(a)). In fact, angle at the hump if the new center-of-gravity position does not produce undesirable stability characteristics.

CONCLUDING REMARKS

The selection of the best of these hulls for a given design will probably be governed by considerations

14.5 f. p. s.; $\tau=7°$; $\Delta=40$ lb. | 13.9 f. p. s.; $\tau=7°$; $\Delta=40$ lb. | 13.4 f. p. s.; $\tau=7°$; $\Delta=40$ lb.

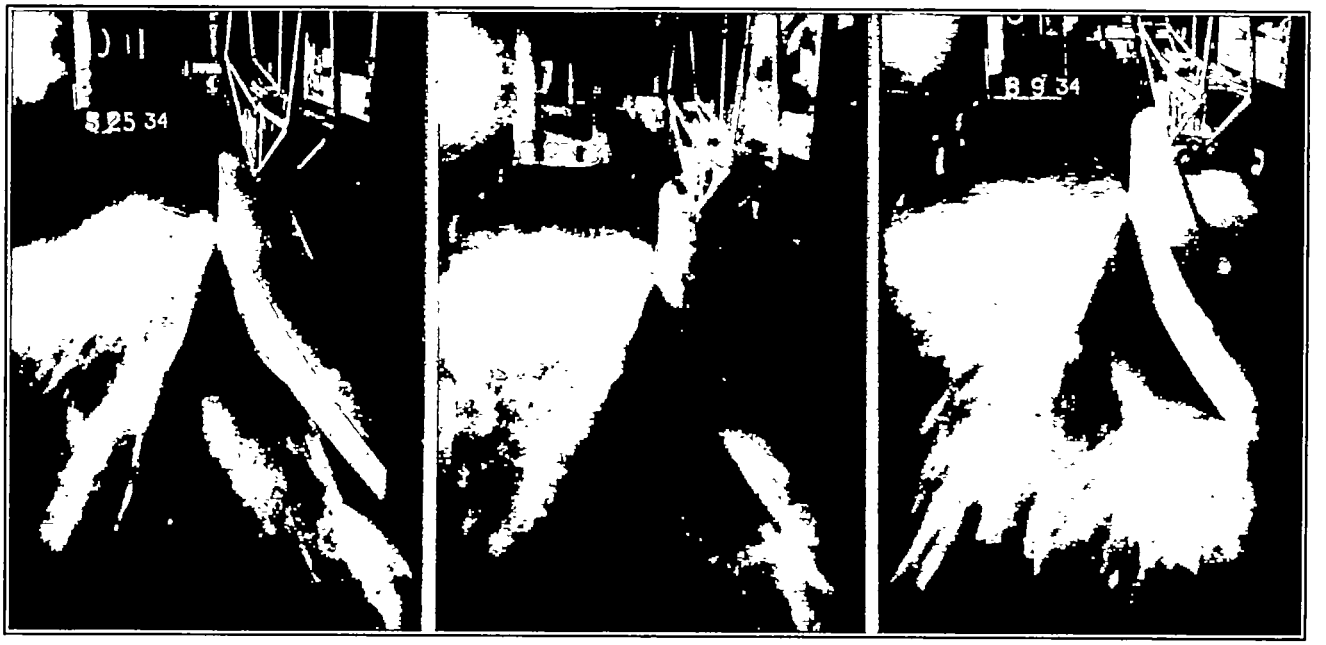

19.7 f. p. s.; $\tau=7°$ $\Delta=80$ lb. Model 40AC, pointed afterbody. | 19.5 f. p. s.; $\tau=7°$; $\Delta=80$ lb. Model 40AD, second-step afterbody. | 18.4 f. p. s.; $\tau=7°$; $\Delta=80$ lb. Model 40AE, no-step afterbody.

FIGURE 72.—Effect of afterbody form on spray pattern. Normal forebody.

the critical peak of the free-to-trim resistance curve can be eliminated by moving the center of gravity sufficiently far aft and accepting the accompanying higher trimming moment required to obtain best trim other than the water-resistance characteristics because of the comparatively small differences in the resistance curves of the five models. Model 40–BE offers least resistance at the hump and model 40–AC the least at

high speeds but, in general, the differences are not sufficiently great to be a determining factor.

The developable forebody apparently offers a satisfactory solution for the problem of simplified construction without an accompanying sacrifice in performance. In the smooth water of the tank there was little choice between the two forebodies in regard to the spray. In rough water the developable forebody would probably have slightly poorer spray characteristics than the other forebody.

It is suggested that the spray strips be continued forward until they meet at the bow.

It appears from the take-off examples that the margin of excess thrust is likely to be less near get-away speed than it is at the hump. Exceptions to this statement may be found when controllable propellers and/or very low wing loadings are used. An increase in the load coefficient will usually raise the hump $R+D$ and lower the high speed $R+D$ but, in the case of these models, it is not recommended that the initial load be increased beyond the maximum load tested because the spray may become excessive, particularly at the bow. In fact, if very rough water is to be encountered in service it would appear advisable to use only a moderately high load coefficient.

It should be possible to use even greater angles of afterbody keel than were used in the present case without greatly increasing take-off time or run. In fact, there may be an appreciable improvement if the high-speed resistance is critical. (See reference 5.)

LANGLEY MEMORIAL AERONAUTICAL LABORATORY,
NATIONAL ADVISORY COMMITTEE FOR AERONAUTICS,
LANGLEY FIELD, VA., *June 19, 1935.*

REFERENCES

1. Truscott, Starr: The N. A. C. A. Tank. A High-Speed Towing Basin for Testing Models of Seaplane Floats. T. R. No. 470, N. A. C. A., 1933.
2. Shoemaker, James M.: Tank Tests of Flat and V-Bottom Planing Surfaces. T. N. No. 509, N. A. C. A., 1934.
3. Shoemaker, James M., and Parkinson, John B.: A Complete Tank Test of a Model of a Flying-Boat Hull—N. A. C. A. Model No. 11. T. N. No. 464, N. A. C. A., 1933.
4. Hartman, Edwin P.: Working Charts for the Determination of Propeller Thrust at Various Air Speeds. T. R. No. 481, N. A. C. A., 1934.
5. Allison, John M.: The Effect of the Angle of Afterbody Keel on the Water Performance of a Flying-Boat Hull Model. T. N. No. 541, N. A. C. A., 1935.

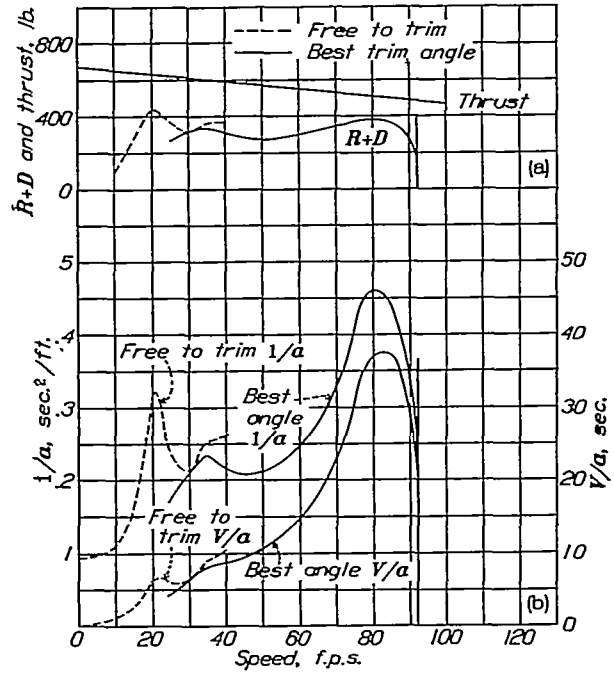

FIGURE 75.—Curves for determining take-off time and run for the 2,000-pound example.

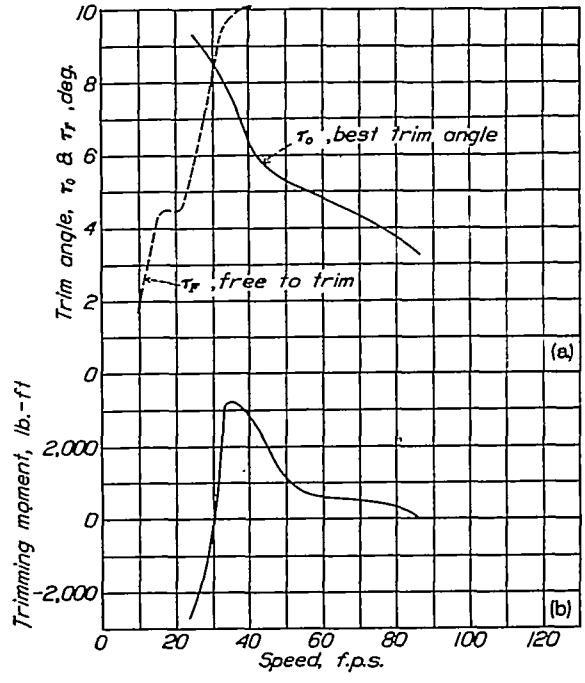

FIGURE 76.—Trim angle and trimming moment curves for the 2,000-pound example. Δ=80 lb.

TABLE I.—OFFSETS FOR FOREBODY A, INCHES

Station	Distance from F. P.	Distance below base line						Half-breadths					
		Keel	B 1, 1.30[1]	B 2, 2.60	B 3, 3.90	B 4, 5.20	Chine	Chine	WL 1, 12.40[2]	WL 2, 10.80	WL 3, 9.20	WL 4, 7.60	WL 5, 6.00
F. P.	0	Tangent at 4.00					4.00	Tangent					
¼	1.05	7.79	5.40				4.84	2.07				0.16	0.85
½	2.10	9.24	6.96	5.81			5.66	2.92			0.12	.87	2.27
1	4.20	11.01	9.22	7.89	7.16		7.13	3.99		0.23	1.32	3.00	
1½	6.30	12.13	10.71	9.48	8.67		8.38	4.74		1.23	2.99		
2	8.40	12.86	11.74	10.67	9.88	9.40	9.63	5.29	0.57	2.44			
3	12.60	13.66	12.90	12.12	11.44	10.92	10.64	5.98	2.11	5.46			
4	16.80	13.95	13.39	12.81	12.25	11.75	11.31	6.33	3.54				
5	21.00	14.00	←	—	—	→	11.59	6.46					
6-10	25.20-42.00	14.00	←	—	—	→	11.67	6.50					

[1] Distance from center line (plane of symmetry) to buttock (section of hull surface made by a plane parallel to plane of symmetry).
[2] Distance from base line to water line (section of hull surface made by a horizontal plane parallel to base line.)

TABLE II.—OFFSETS FOR FOREBODY B, INCHES

Station	Distance from F. P.	Distance below base line						Half-breadths					
		Keel	B 1, 1.30	B 2, 2.60	B 3, 3.90	B 4, 5.20	Chine	Chine	WL 1, 12.40	WL 2, 10.80	WL 3, 9.20	WL 4, 7.60	WL 5, 6.00
F. P.	0	Tangent at 4.00					4.00	0.10					
¼	1.05	7.36	5.19				4.75	1.45					0.90
½	2.10	8.83	7.37				5.54	2.46				1.13	2.21
1	4.20	10.72	9.70	8.46			7.06	3.84			1.85	3.39	
1½	6.30	11.91	11.09	10.12	9.08		8.37	4.72		1.70	3.75		
2	8.40	12.69	11.99	11.19	10.35	9.43	9.36	5.29	0.59	3.22			
3	12.60	13.55	12.99	12.37	11.75	11.05	10.64	5.98	2.53	5.68			
4	16.80	13.88	13.42	12.88	12.34	11.79	11.31	6.33	3.74				
5	21.00	14.00	13.54	13.06	12.57	12.07	11.59	6.46	4.32				
6-10	25.20-42.00	14.00	←	—	—	→	11.67	6.50					

TABLE III.—OFFSETS FOR AFTERBODY C, INCHES

[Elements of stations are straight lines]

Station	Distance from station 10A	Distance below base line				Half-breadths	
		Keel	Main chine	Cove	Upper chine	Main chine and cove	Upper chine
10A	0	13.50	11.17			6.50	
11	4.2	↑	10.62			6.50	
12	8.4		10.08			6.47	
13	12.6		9.55	7.09	7.09	6.39	6.39
14	16.8		9.13	6.56	6.49	6.04	6.23
15	21.0		8.89	6.20	5.91	5.18	5.98
16	25.2		8.84	6.05	5.36	3.77	5.68
17	29.4	↓	8.95	6.04	4.83	1.97	5.30
18F	33.0	9.15	9.11	6.11	4.41	.20	4.89
18A	33.0	6.15			4.41		4.89
19	38.0	↑			3.86		4.22
20	43.0				3.35		3.44
21	48.0				2.83		2.54
22	53.0	↓			2.46		1.52
23	58.0	2.19			2.08		.40

TABLE IV.—OFFSETS FOR AFTERBODIES D AND E, INCHES

[Elements of stations are straight lines]

Station	Distance from station 10A	Chine half-breadth	Distance below base line			
			Afterbody D		Afterbody E	
			Keel	Chine	Keel	Chine
10A	0	6.50	13.50	11.17	13.50	11.17
11	4.2	6.50	↑	10.54	↑	10.54
12	8.4	6.47		9.93		9.93
13	12.6	6.30		9.33		9.33
14	16.8	6.23	↓	8.76		8.76
15	21.0	5.98	10.36	8.22		8.22
16	25.2	5.68	9.80	7.77		7.71
17	29.4	5.30	9.37	7.48		7.22
18F	33.0	4.89	9.15	7.41		6.83
18A	33.0	4.89	8.57	6.83		6.83
19	38.0	4.22	↑	6.32		6.32
20	43.0	3.44		5.85		5.85
21	48.0	2.54		5.44		5.44
22	53.0	1.52	↓	5.06	↓	5.06
23	58.0	.40	4.83	4.72	4.83	4.72